Direct Matching Antennas in RF Energy Harvesting Systems: A Review

V. Honarvar [1], F. Mohajeri[2*]
1-Department of Electrical and Computer Engineering, Shiraz University, Shiraz, Iran.
Email: vhonarvar@gmail.com (PhD Student)
2-Department of Electrical and Computer Engineering, Shiraz University, Shiraz, Iran.
Email: mohajeri@shirazu.ac.ir (Corresponding author)

Received: 17 September 2022 Revised: 12 October 2022 Accepted: 22 November 2022

ABSTRACT:
A historical review of Radio Frequency Energy Harvesting (RFEH) Rectenna (Rectifier Antenna) Systems without a matching network is performed, with emphasis on the antenna part. As the antenna, matching network and rectifier are the main parts of the rectenna systems, the reasons behind the elimination of the matching network are presented and different special antennas suitable for direct matching to the rectifier, without using a matching network, are reviewed. Since the diode in the rectifier is a nonlinear element, its input impedance is changed with varying operating conditions such as input power, frequency and output load impedance of the rectifier. So, it is a challenge for researchers to match the antenna impedance directly to the rectifier in variable operational conditions.

KEYWORDS: RF Energy Harvesting (RFEH), Rectenna, Elimination of Matching Network, Non-50Ω antennas.

1. INTRODUCTION

Powering remote devices and sensors in the Internet of Things (IoT) enabled devices, Wireless Sensor Networks (WSN), wearable and implantable systems and other similar applications are emerging challenges and it has been reflected in designing more reliable devices and systems. One of the promising solutions for this subject is Radio Frequency Energy Harvesting (RFEH) and Wireless Power Transfer (WPT). In these solutions, a rectenna (rectifier-antenna) [1] is used to receive and convert the RF wireless energy to a DC signal useful for powering remote devices [2-7]. An energy harvesting circuit can be seen in Fig. 1. Two key parameters of the rectenna in the mentioned applications are compactness and being able to convert available low levels of energy efficiently [8], [9].

In applications that receive ambient RF energy, the amount of available RF power density is very low (at the level of a few $\mu W/cm^2$) [6], [10-13]. One method is to use large antennas to receive the required amounts of energy for the harvesting circuit to operate. But since the rectenna should be compact in many applications, the antenna cannot be large to receive high amounts of energy. So, for utilizing the low amount of received power in the best way, it is important to design a rectenna with high total efficiency and minimum losses.

For the reduction of losses and increase the efficiency in the rectenna, the rectifier and antenna impedances should be matched for maximum power transfer. So, a matching circuit between these parts is proposed [3], [6], [10], [13-27]. But this matching circuit itself introduces extra losses and also increases the size of the rectenna. In fact, it has been shown that for obtaining maximum achievable efficiency in low power conditions, the matching circuit should be removed [28-29], which is also in favour of rectenna size reduction.

With removing the matching circuit, the antenna and the rectifier impedances should be directly conjugate matched for maximum power transfer. This is another important challenge since the diode-based rectifier is a nonlinear device and its input impedance varies with operating conditions (input power level, frequency and output load impedance) [14],[16],[30-35]. So, designing special non-50Ω antennas that are directly matched to the rectifier is an important issue and there have been considerable efforts around it.

This paper reviews the important research done on the direct matching rectennas with an emphasis on the antenna part. Several solutions to this problem in different operating conditions are presented briefly, which can be used for comparing the systems, understanding the pros and cons of each one and choosing the best solution for a specific application. Section 2 reviews non-50 Ω antennas used in the rectenna systems in the literature. In section 3 a

Paper type: Review paper
DOI: 10.30486/mjee.2022.696517
How to cite this paper: V. Honarvar and F. Mohajeri, "Direct Matching Antennas in RF Energy Harvesting Systems: a Review", Majlesi Journal of Electrical Engineering, Vol. 16, No. 4, pp. 61-87, 2022.

comparison of solutions is presented, followed by discussion and conclusion sections at the end.

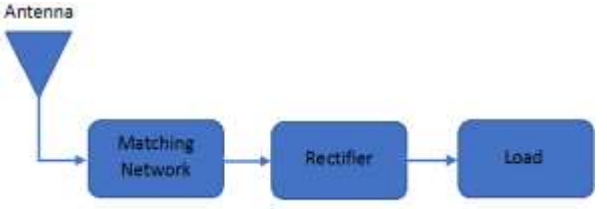

Fig. 1. An energy harvesting circuit or rectenna, including antenna, matching network, rectifier and load.

2. ANTENNAS OF RECTENNA SYSTEMS WITHOUT MATCHING CIRCUIT

Here, research that considers the rectenna design without matching circuits is presented in chronological order to understand the trend of improvements in this area. The key features of each study are mentioned briefly to help get a general familiarization with the ideas involved. Each of the following studies has been performed in different conditions and for different applications, but all of them have considered the elimination of the matching network, which is usually placed between the antenna part and the rectifier part of the rectenna for simplification, size, cost and loss reduction and efficiency improvement. The summarized data for operating conditions and results of each research can be seen in Table 1 at the end of the reviews.

2.1. Early works (2000-2010)

The study of early works begins with [36], in which two non-resonant antenna arrays without a matching network are designed and used in the rectenna system: a dense grid array and a self-similar spiral array. An approach for incident waves of arbitrarily and time-varying polarization and with broad spectral content is presented. This idea is tested on the first antenna that receives two orthogonal linear polarizations (Fig. 2a), and on the second one with alternating right-hand and left-hand circular polarizations (RHCP and LHCP) (Fig. 2b). Although in these rectenna arrays, the antennas are nonresonant and there are no matching circuits, but there are no discussions about the antenna and rectifier impedances and the procedure of direct matching of the antenna array to the rectifier.

In [11], the usefulness of a proposed rectenna in low input power densities and wide frequency range is examined. The proposed rectenna consists of a 64-element dual Circular Polarization (CP) spiral array with each element directly connected to a rectifying diode (Fig. 2c). The frequency-independent antenna (Spiral) is used to enable matching to the rectifier, reducing the overall size and increasing the bandwidth of the system.

A frequency domain Harmonic Balance (HB) method for analyzing nonlinear aspects of the rectifying diode is used. The optimum source impedance range of the diode is determined by the source-pull technique in a range of input powers and frequencies. This optimum source impedance region is then used for optimizing the antenna design. The antenna is designed so that its input impedance matches with the optimum diode source impedance in the desired frequency and mismatches to reflected harmonics (harmonic rejection). For the low-power conditions, it is shown that the SMS7630 Schottky diode has the best performance over the specified frequency range.

Also, different DC power combining schemes are examined and it is shown that for an 8×8 array, the parallel combination of the cells provides the best efficiency in the incident power density range. The other test is performed for single-tone and multi-tone input signals to show that when multiple waves with several frequencies are incident simultaneously, the DC output is increased.

A review of methods of designing UHF passive tag antennas for RFID (Radio Frequency Identification) applications is done in [37]. The design goal of the antenna is: 1) to have inductive input impedance so that it can be conjugately matched to the RFID microchip (for eliminating the matching network), and 2) to miniaturize the antenna shape and size.

For the first goal, the antenna input impedance can be modified by techniques like some modifications on the T-match, coupling to a small loop, and adding nested slots. The second goal (size reduction) is achieved by meandering and inverted-F configurations (inverted-F antenna, IFA and planar inverted-F antenna, PIFA). So, conjugate impedance matching to RFID electronics in conjunction with size reduction of the antenna is achieved by modifying the original antennas using the above-mentioned techniques (See Fig. 3).

In [45] an S-shaped folded dipole antenna (Fig. 4a) and an inductively coupled feed antenna (Fig. 4b) are introduced, which the first one has 2 matching stubs (resistive and inductive) as parts of the antenna, but the second antenna has no matching circuit attached. These antennas are proposed for use in ultra-compact RFID designs.

Antennas are designed to be conjugately matched with RFID IC with the capacitive input impedance of $Z_{IC} = 73 - j113\ \Omega$. This article mainly discusses antennas suitable for RFID Tags, and is not about the complete rectenna system.

A meandered slot dipole antenna is proposed in [46] with no matching network (Fig. 4c). According to Babinet's principle, a slot dipole antenna has the property of impedance transformation with respect to the dipole antenna.

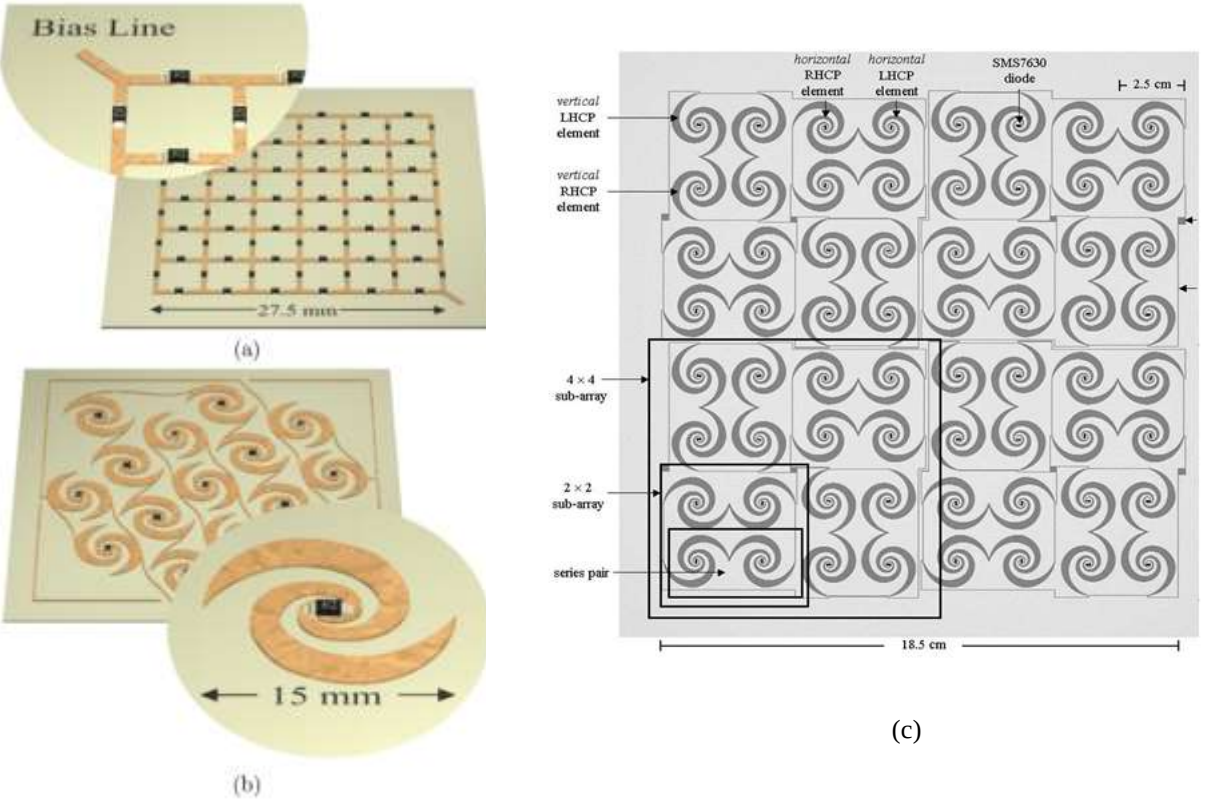

Fig. 2. (a) The grid array, (b) the spiral array [36], and (c) the Layout of the 64-element spiral array [11].

The antenna is designed so that it is conjugately matched to the specific RFID tag chip (with a 20-j135 Ω impedance). The impedance of the antenna can be tuned by changing horizontal and vertical lengths (L_v and L_h) of the conductor area.

To design a low-cost rectenna in low input power conditions, in [47] a rectenna is designed using analytical models and closed-form expressions. A probe-fed microstrip patch antenna (Fig. 5a) whose input impedance varies with the probe position is used to perform direct matching to the rectifier. Although matching circuits are not used in this design, input and output filters (as radial stubs) are used for preventing the RF signal or its harmonics from being propagated to the input antenna or output load. This is in contrast to the compactness of the rectenna.

In [48], some improvements to [47] are realized as follows (Fig. 5b):

1-Changing the excitation method of the microstrip antenna from probe feeding to edge feeding. This modification leads to the ability to fabricate the whole rectenna on a single side of a grounded printed circuit board (PCB).

2- There is no need to use a transmission line stub as a harmonic filter since the patch antenna is a narrow-band device and is mismatched to the higher order harmonics generated by the rectifier inherently. So, the stub can be omitted.

3- The filter used between the rectifier and load also can be omitted, since it is stated that this will not affect the rectenna performance seriously.

With the above improvements, higher efficiency with respect to [47] (about 52%) is obtained.

In [49], to maximize RF-to-DC conversion efficiency and ensure the compact physical dimensions of rectenna, impedance matching and filtering networks are not employed. A wire Folded Dipole Array (FDA) antenna is chosen (Fig. 5c) since its geometry has enough parameters to tune its input impedance for direct matching to the rectifier.

An analytical model and approximation method are used to find antenna input impedance in terms of its geometrical parameters. The RF input impedance of a specific diode (HSMS-2850) has been determined by

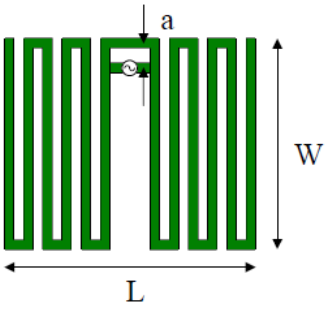

(a)

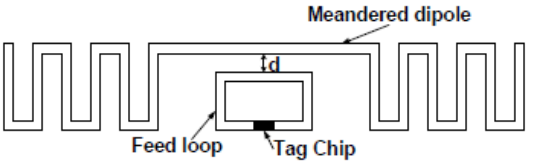

(b)

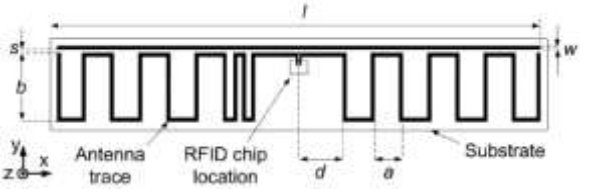

(c)

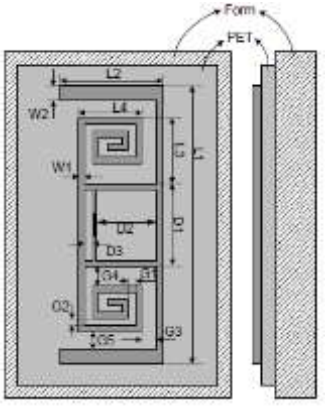

(d)

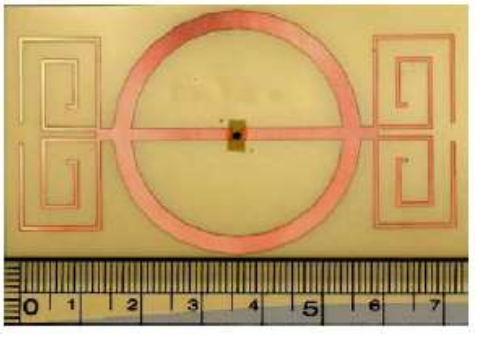

(e)

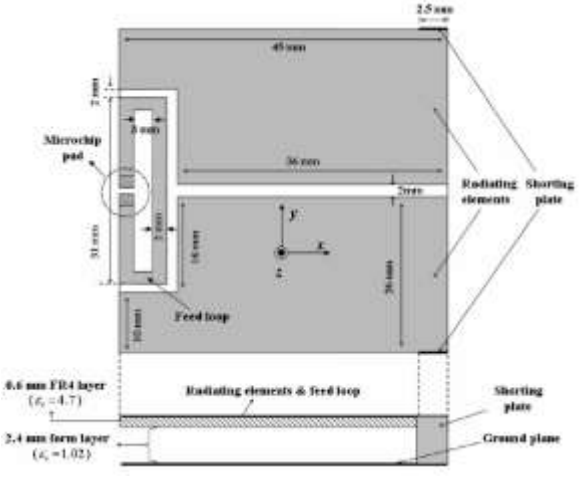

(f)

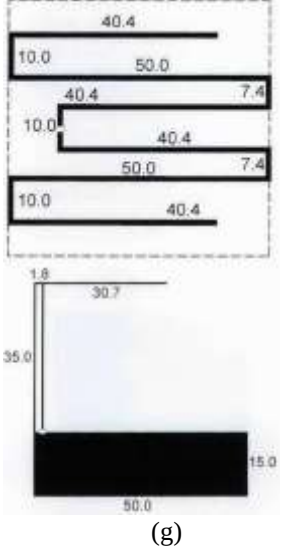

(g)

Fig. 3. Meander-line antennas equipped with a T-match feed in (a) [38], with an inductively coupled loop feed in (b) [39], and with a loading bar in (c) [40], [41]; (d) a multiconductor antenna equipped with a double T-match and spiral folding [42], (e) a multiconductor meander-line antenna equipped with a circular double T-match [43], (f) the proximity loop feed in a two-layer double-PIFA tag [44], (g) a meander-line with an inverted-F antenna optimized with a genetic algorithm [37].

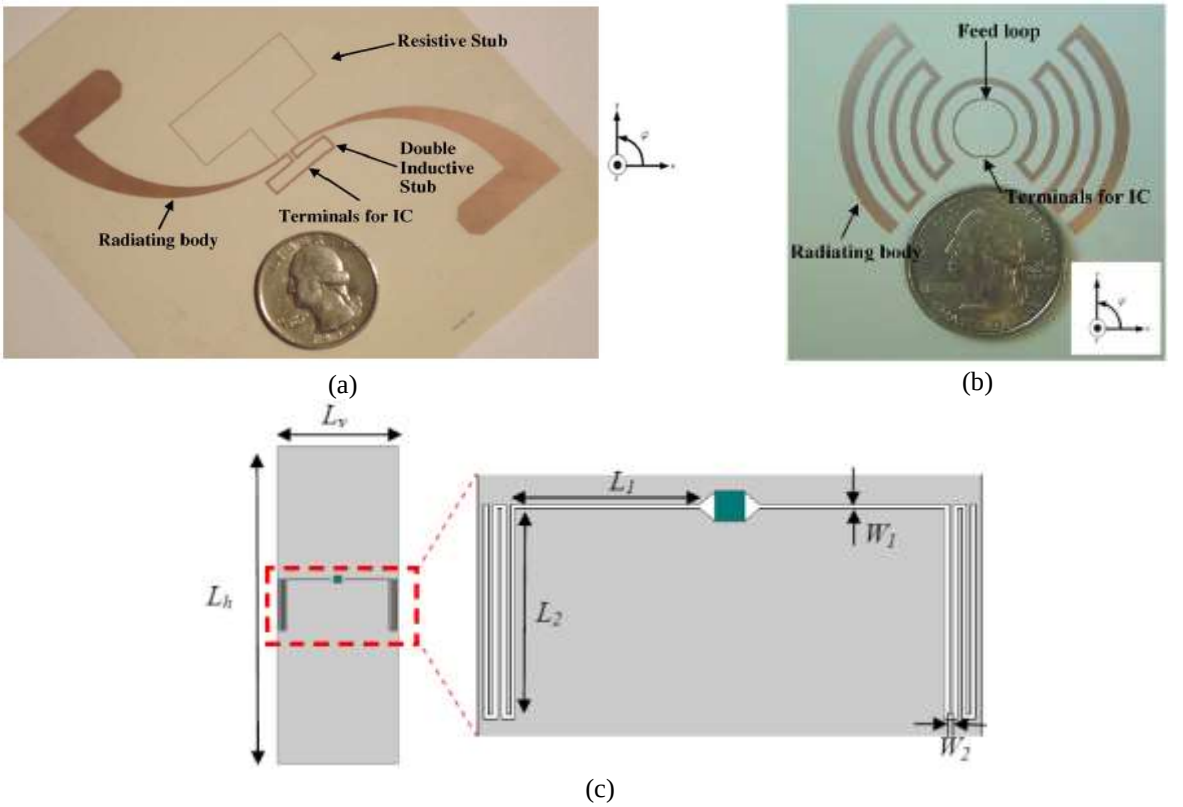

Fig. 4. (a) S-shaped folded dipole antenna structure showing stubs [45], (b) inductively coupled feed antenna [45], (c) layout of the meandered slot dipole antenna with chip boundary [46].

Using a Runge-Kutta (RK) method for a short circuit load at specific input power and frequency.

The input impedance of the antenna as a function of its geometrical parameters is then embedded in a custom-made Genetic Algorithm (GA) optimization shell, with a fitness function that is related to the power reflection coefficient between the antenna and the diode. So, the geometrical parameters of the antenna that minimize the power reflection coefficient can be found. In this way, the best conjugate matching between the antenna and the diode is achieved. Also, it is stated that the proposed analysis method of antenna input impedance has good agreement with the Method of Moment (MoM) method results, with much less computation time.

2.2. Research done from 2011-2018

A meandered slot antenna (Figs. 5d ad 5e) is designed in [50] by Genetic Algorithm Optimization (GAO) at 2.45 GHz to maximize conjugate matching to an RFID chip with known input impedance. It is shown that utilization of GAO in the design of this antenna can also reduce the antenna size.

In [51], a metamaterial-inspired near-field resonant parasitic (NFRP) antenna is directly matched to the rectifier in the L1 frequency band of the GPS (Global Positioning System) application. A metamaterial-inspired S-shaped NFRP element is combined with a driven printed monopole element with a two-cane top-loading, to achieve an Electrically Small Antenna (ESA) structure (Figs. 5f and 5g). An input DC block Band Pass Filter (BPF) and output Low Pass Filter (LPF) (inductor) are used for preventing DC and harmonic frequency components to be reached to input antenna and output load, respectively.

The rectifier is analyzed by source-pull and load-pull techniques in Advanced Design System (ADS), and its optimal load and the input impedance are determined, which yields antenna input impedance for conjugate matching. The antenna was designed using a High-Frequency Structure Simulator (HFSS). Since the ratio of the reactance to the resistance of the antenna is found to be high, the driven printed monopole with a two-cane top-loading is used to achieve this high impedance ratio.

Source-pull and load-pull techniques are also used in [52], to find the optimal diode RF and dc (input and output) impedances for the most efficient rectification, as a function of input power. A Harmonic Balance simulation is utilized to find the optimum input impedance of a specific diode for a given dc load resistance, input power and frequency.

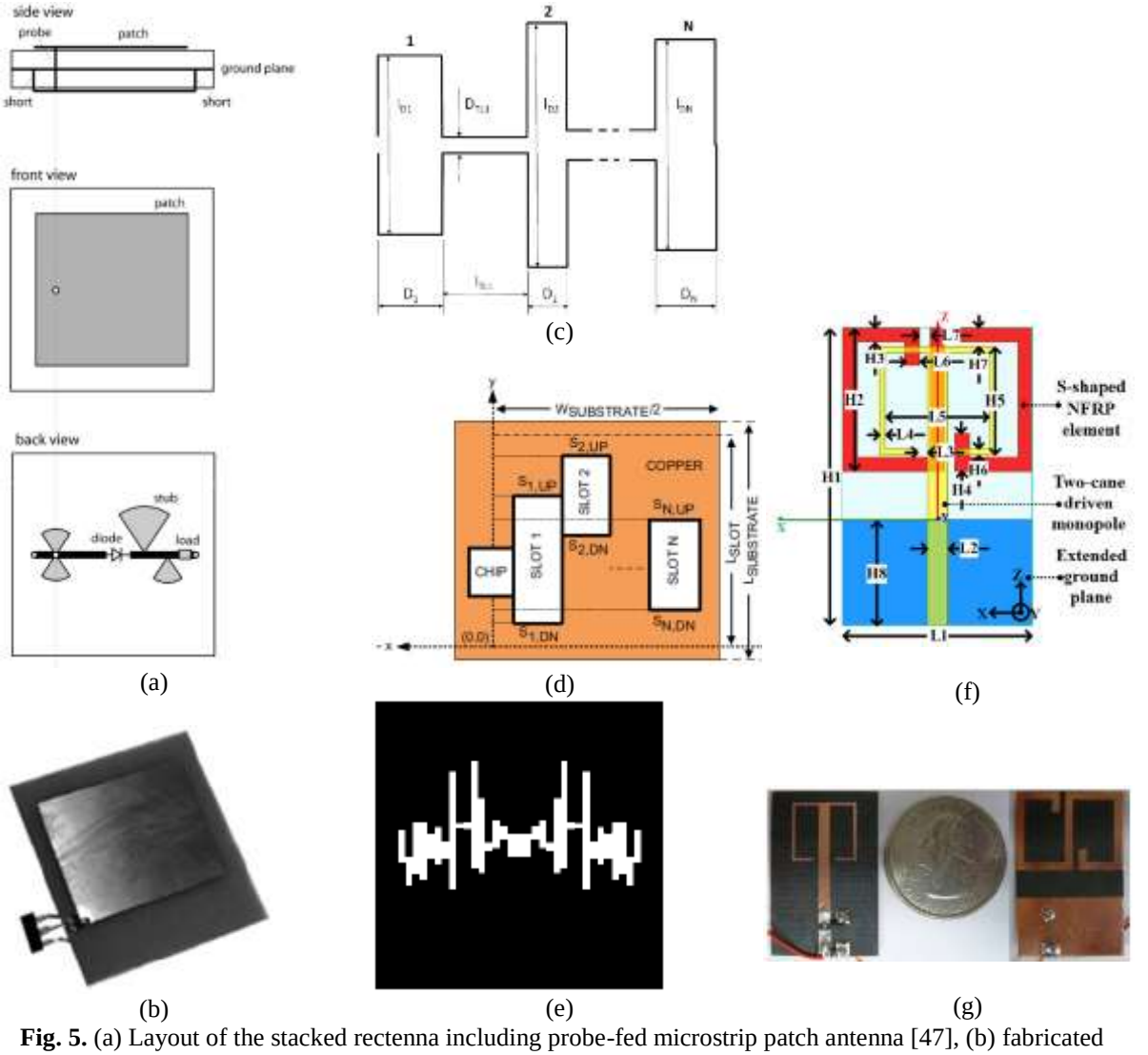

Fig. 5. (a) Layout of the stacked rectenna including probe-fed microstrip patch antenna [47], (b) fabricated edge feed microstrip patch antenna in a single-layer grounded PCB rectenna [48], (c) N-elements wire FDA antenna [49], (d) generic layout of meandered slot antenna [50], (e) optimized meandered slot antenna layout for known input impedance [50], (f) layout of the GPS L1 antenna [51], (g) fabricated GPS L1 rectenna front and back views: two-cane driven monopole with rectifying circuit (left), S-shaped NFRP element with the extended ground plane (right) [51].

A source-pull measurement is then performed to validate the simulation results. By repeating this procedure, the mentioned optimum RF and DC impedances of the diode are obtained.

This allows optimized antenna design, in which its input impedance gives the best possible match to the rectifier and so the best conversion efficiency can be obtained. This process can eliminate or simplify match networks and improve overall efficiency. Because of limitations in designing of proper antenna that is directly matched to the rectifier and hence omitting the matching circuit completely, the results are used to design the antenna that simplifies the matching circuit (Fig. 6b) with the goal of good efficiencies. It is mentioned that complete elimination of the matching network might be possible with other antennas and diodes.

A patch antenna with different widths and feed points (Fig. 6a) is simulated and measured to find the impact of the width of the patch, location of the feed and parasitic of the antenna connector on the antenna input impedance. It is shown that the antenna impedance (especially its reactance) is highly sensitive to the parasitic of the feed connector. The power densities of interest in this practice are relatively low (25 to 200 $\mu W/cm^2$).

In [53], a co-design is made on a single band, compact and high gain X-shape antenna with a stub (Fig. 6c) and a rectifier, so that they directly match each other

at the main frequency, while they are mismatched at higher order harmonics. This prevents the use of a BPF between the antenna and the rectifier for rejecting higher-order harmonics. The stub length controls the antenna input impedance for best matching with the rectifier. As another feature, this antenna has a 60 degrees half-power beamwidth (HPBW), which is an advantage because there is no need to perform precise alignment of the rectenna to the power sources to receive enough power and maintain the conversion efficiency.

It is shown that the efficiency is sensitive to the values of the load resistor. In the input power range larger than -15 dBm, the efficiency is lower with larger load resistances. The maximum achieved efficiency is 83% for a load resistance of 1400 Ω at 0 dBm input power.

Another rectenna system is considered in [54] without a bandpass filter and impedance matching circuit, using a circular sector antenna (Fig. 6d) with harmonic-rejecting characteristics. Direct matching with a double diode rectifier is achieved by tuning the impedance of the antenna by varying its feeding points. The antenna and the rectifier are built on both sides of the board for size reduction. A common ground plane is placed between these two layers. An LPF is used between the rectifier and load for DC passing.

In [55], the co-design of a multi-stage CMOS rectifier and a compact square loop antenna with additional short-circuited arms (Fig. 6e) for an RF energy harvester in a Wireless Sensor Network (WSN) application is presented. The input impedance of the 5-stage CMOS rectifier is simulated and then the specialized loop antenna dimensions are adjusted so that it is conjugately matched to the rectifier. It is mentioned that at low input powers (near the diode turn-on threshold) the input impedance of the rectifier is dominated by the linear parasitic components, and so the real and imaginary parts of rectifier input impedance can be considered constant. A cross-connected differential rectifier is used, which its capacitive input impedance is compensated by using an antenna with an inductive reactance.

In [56], a flexible low-mass printed rectenna is designed. The voltage and current waveforms in the diode are shaped using a time-domain waveform shaping method so that its conversion efficiency is maximized. By direct matching of the rectifier and antenna at a given frequency and input power, the matching network is omitted and so the rectenna size is reduced. By using class-F terminations in the rectifier at the harmonics of the operating frequency (in which even harmonics are terminated in short circuits, while odd harmonics are terminated in open circuits), the efficiency of the rectifier is improved. A coplanar dipole antenna is integrated with the compact meandered feed line to build the mentioned harmonic terminations. A gap is included to block DC and a capacitor is used to short the even harmonics. The antenna is equipped with a shorted quarter-wavelength Coplanar Strip line (CPS) stub which is a short circuit at even harmonics due to the capacitor and an open circuit at f_0 and odd harmonics (See Figs. 7a and 7b).

Another low-mass rectenna is introduced in [9], which has high efficiency at very low power densities at two specified frequencies (2.45 GHz and 915 MHz) and a given DC load (2.2 KΩ).

A three-element Yagi-Uda antenna (Fig. 7c) is designed so that it is directly matched to the rectifier at 2.45 GHz. Assuming 1 μW/cm^2 input power density, and using SMS7630 Spice model parameters, source-pull simulations were performed to find the optimized impedance that should be presented to the diode to give the highest DC voltage across the fixed load. Since this optimal impedance is inductive, it is obtained by using an inductive feed method inspired by the design of RFID tags [37].

A dc collection network (two serial short-circuited quarter-wavelength CPS) is designed to isolate the dc load from the antenna. These CPS lines are open circuits at the diode feed point (at 2.45 GHz) but provide a path to deliver power to the dc load. An RF-short capacitor (in 2.45 GHz) is added to ensure RF-dc isolation. The antenna is designed to be directly matched to the rectifier at 2.45 GHz. But at 915 MHz, the matching is performed with the help of the mentioned CPS stubs, which are inductive and not open circuits at 915 MHz, and the RF capacitor, which is not a short circuit in this frequency.

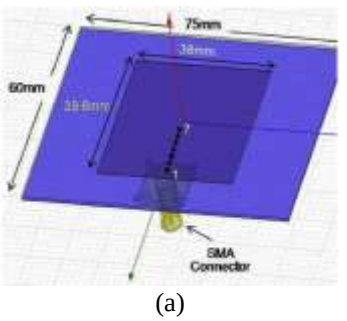

(a)

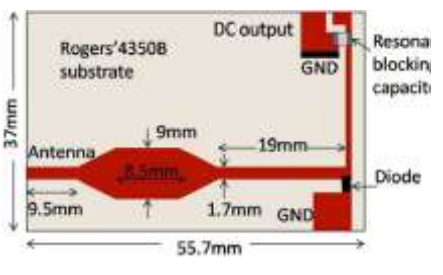

(b)

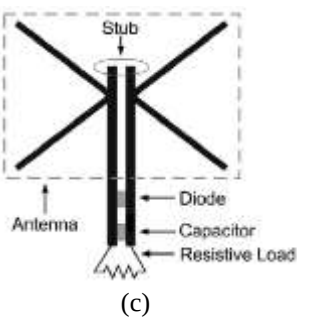

(c)

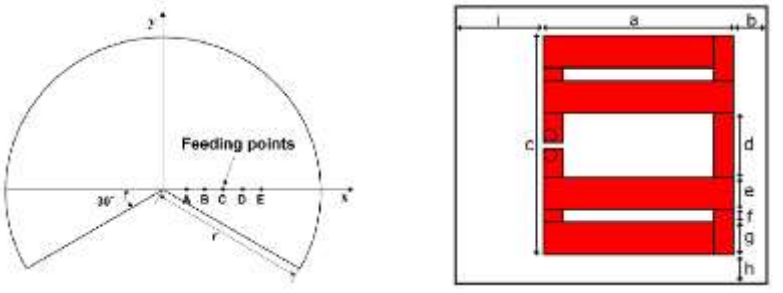

(d) (e)

Fig. 6. (a) Geometry of patch antenna with seven feed points [52], (b) layout of the matching circuit used [52], (c) circuit configuration of the rectenna including the X-shape antenna with a stub [53], (d) layout of the circular sector antenna with different feeding points [54], (e) square loop antenna with short-circuited arms [55].

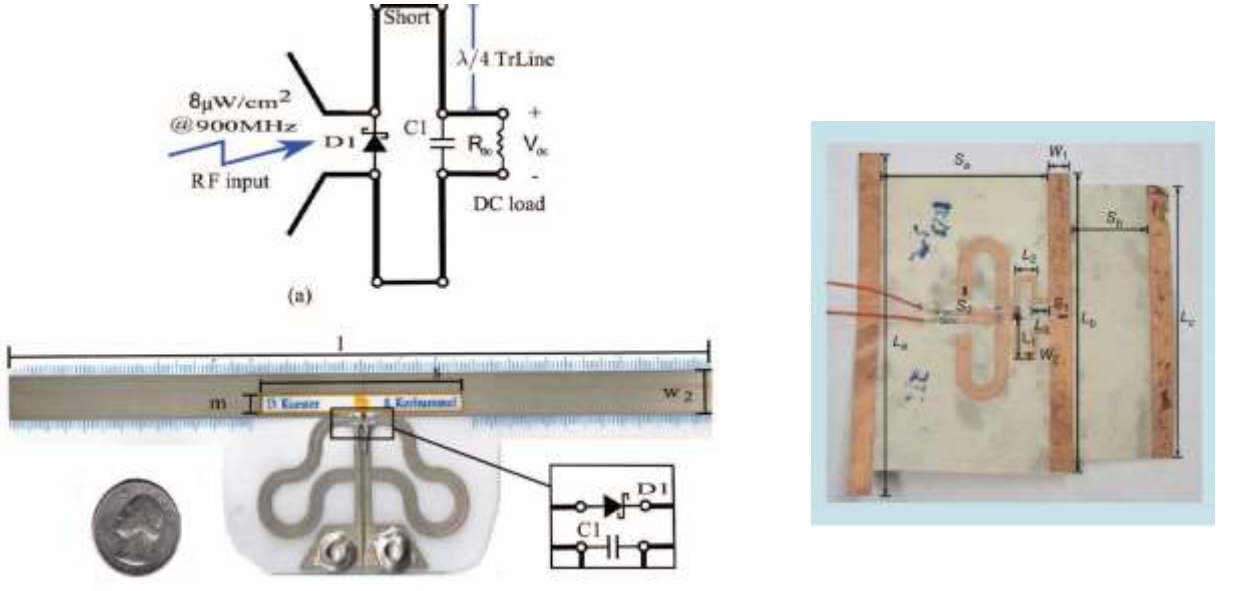

(b) (c)

Fig. 7. (a) Circuit diagram of rectenna in [56], (b) photograph of the flexible rectenna [56], (c) the manufactured prototype rectenna including a three-element Yagi-Uda antenna [9].

In [57] and [28], a rectangular loop-like printed antenna with additional short-circuiting arms (Fig. 8a) is introduced, which is directly matched to a voltage doubler rectifier. Considering the input impedance of the rectifier under operating conditions, the input impedance of the desired antenna must be inductive with a small resistive part, and this is achieved by tuning the geometrical features of the mentioned antenna. The results are also compared to a similar rectenna with a 50 Ω antenna and lumped elements matching network, which shows around 5% efficiency improvement in conjugate matching rectenna. The reason is mentioned to be the losses of the matching circuit.

A folded dipole antenna equipped with an inductive feed and a corner reflector (Fig. 8b) is studied in [8] with two different diodes (VDI ZBD and Skyworks SMS7630-079). The optimum impedance needed for maximum efficiency is calculated by load-pull simulation under operating conditions. It is found that for the VDI ZBD diode, a high impedance is needed for direct matching, which is difficult to achieve. But for the Skyworks SMS7630-079, the needed impedance can be achieved more easily. It should be mentioned that because of the characteristics of the utilized antenna, an inductive matching (feed) is used instead of direct matching.

In [58], a broadband antenna with both vertical and horizontal polarizations is designed and used with a

voltage doubler rectifier for energy harvesting. For increasing the bandwidth and maintaining a large beamwidth, the structure of the antenna is optimized by gradual flaring of each bend of the antenna (Fig. 8c). It is mentioned that since the rectifier input impedance changes with frequency, input power and load, so the antenna should be designed such that it has a frequency broad band impedance match for a given input power range and a particular load value.

In the design procedure of the rectenna, first, the behaviour of the diode input impedance is studied with various dc loads, input frequencies and input power levels. It is found that the best efficiency performance, which is obtained in 500 Ω load, is not a strong function of the frequency, and so it is possible and useful to design a broadband antenna matched to the optimum rectifier input impedance. The optimum impedance of the rectifier is found to be a real value dominantly (100 Ω) and the imaginary part is negligible.

In [59], a 3-D vertical stack of 4×4×4 folded dipole antennas (FDA) (Figs. 8d, 8e and 8f), each of which directly connected to a single diode rectifier, is introduced. The stacked rectenna arrays or panels are connected in various ways (series, parallel and hybrid) to channel the collected power to a single DC load, so the DC power combining circuitry is used. The optimum DC load is different with each of the power combining schemes.

In the design procedure, the single diode rectifier input impedance is first calculated by considering a specific (300 Ω) load. Then the antenna sizes are tuned to have a conjugate input impedance with respect to the diode. Then the stacked array of antennas is formed with DC combining schemes. It is mentioned that the mutual coupling effects between antennas are of low importance. It is shown that with the stacked array, the power absorption enhancement (PAE) is 5 times higher than in a single 4×4 array.

In [60], a multiband rectenna, consisting of four-printed-cross-dipole antenna arrays (4CDAA) and a single Schottky diode (Figs. 9a, 9b and 9c), is used to harvest the RF energy from spillover loss of the satellite antennas in Ku and K bands. The system operates at 12 GHz, 17.6 GHz and 20.2 GHz. Based on the explanations, the diode input impedance with a 300 Ω load is around 50 Ω at the mentioned frequencies. So, if we use the standard antenna with an impedance of about 50 Ω at 12 GHz, the matching is achieved. At 2 other frequencies, the matching is also acceptable.

A broadband energy harvesting circuit without using an external matching network, over a wide frequency range (800 MHz to 2.5 GHz) is presented in [61]. The antenna is designed such that its input impedance satisfies the requirements for direct matching to the rectifier. A planar broadband 5-element triangular folded monopole antenna with an input impedance of 300 Ω is designed (Figs. 9d and 9e). The high impedance antenna is used for both direct matching and increasing voltage at the rectifier input. The optimum antenna impedance is found in this way: with a load impedance of 3 KΩ, and the input powers of -5 dBm and -10 dBm, the output power of the rectenna as a function of frequency at different antenna impedances is simulated. It is found that at antenna impedances between 300 to 400 ohms, the output power in the desired frequency range is maximum. So, it is decided to design a broadband antenna with 300 Ω input impedance. This antenna is designed by replacing the unit element of the folded monopole antenna with a triangular monopole element, which is a broadband structure.

In [62], a full-diversity rectenna that its antenna is conjugately matched to the rectifier with a wide frequency band (0.9 to 1.1 and 1.8 to 2.5 GHz), wide input power range (0 to 23 dBm), a wide range of load Values (200 to 2000 Ω), dual-polarization and various rectifier elements (diodes) is proposed

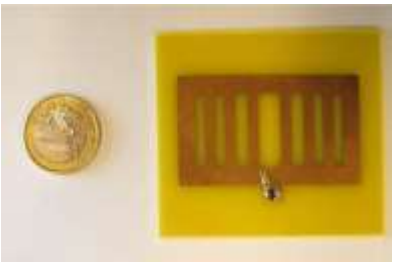

(a)

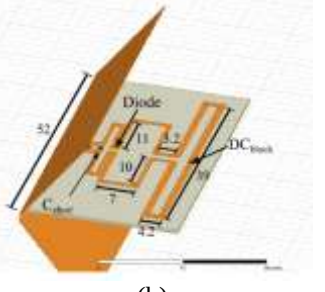

(b)

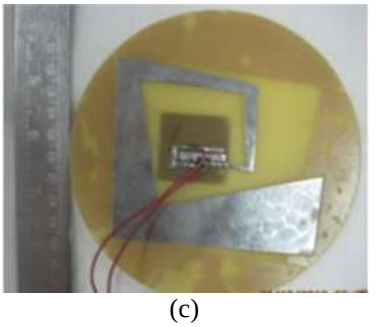

(c)

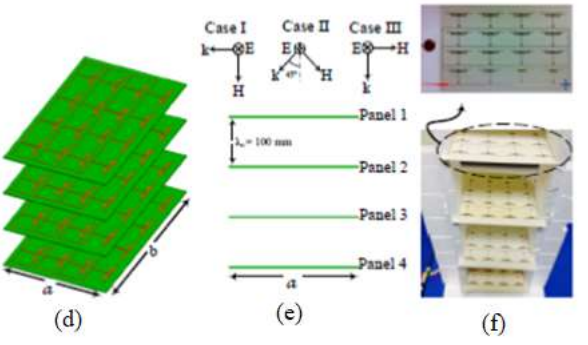

Fig. 8. (a) Realized rectenna consisting of a printed loop-like antenna with short-circuiting arms directly connected to a voltage doubler rectifier [57, 28], (b) rectenna layout with the VDI ZBD diode, including a folded dipole with an inductive feed and a corner reflector [8], (c) fabricated broad band bent triangular antenna [58], Schematic for (d) the 4 vertically stacked panels including FDAs [59], (e) incident plane wave polarization in the system of stacked FDA panels[59], and (f) photograph of 4 stacked panels of FDAs [59].

. It starts with a center-fed half wavelength dipole and makes it off-center-fed to increase the radiation resistance in the first step. Then the bowtie concept is used to increase the frequency band. In the next step, two off-center-fed bowties are crossed to enable dual polarization and a symmetric bowtie is added to control the impedance of the antenna (Fig. 9f). It is shown that the proposed rectenna is broadband and it has good performance in different operating conditions. By choosing different diodes, the optimum input power range can be tuned from 0 dBm to 23 dBm. Also, the conversion efficiency in different conditions can be higher than 60%.

The loss of the matching circuit is studied in [29]. It is shown that the matching circuit in the rectenna should be removed for achieving maximum efficiency in low input power conditions. It is stated that even in a perfect impedance match, if the matching network elements are lossy, up to 95% of power may be dissipated by these elements in ultralow-power conditions. First, maximum achievable power conversion efficiency (PCE) in the -20 to 0 dBm input power range is calculated using an optimization procedure. Optimum values for the load are obtained in each frequency of 900 MHz, 1.8 GHz, 2.4 GHz and 5.8 GHz. It is observed that maximum PCE is achieved in half-wave rectifier topology (which has the minimum number of components) at all mentioned frequencies. Also, it is shown that in the considered input power range, maximum PCE is obtained at 900 MHz. It is seen that in higher frequencies, the optimum input power for maximum PCE is increased. The diode used for rectification is HSMS-286C. The above results are achieved with the assumption of perfect matching. Then for inspecting the effect of the matching circuit, the extra matching circuit loss, G_p, is simulated and measured in 3 types of matching circuits: LC network, single and double-stub tuners on FR4 and Duroid 5880 substrates. It is observed that in the 900 MHz and -20 to 0 dBm input power range, more than 90% and 65% of input power is dissipated in the matching circuit and not delivered to the rectifier, in FR4 and Duroid 5880 substrates respectively. This dissipation is decreased in other higher frequencies, so in 5.8 GHz, the matching circuit loss is less, but on the other hand, the PCE is also decreased as the frequency is increased. So, the loss of the matching circuit is dominated by lower frequencies (e.g., 900 MHz and 1.8 GHz) and low input power conditions (-20 to 0 dBm).

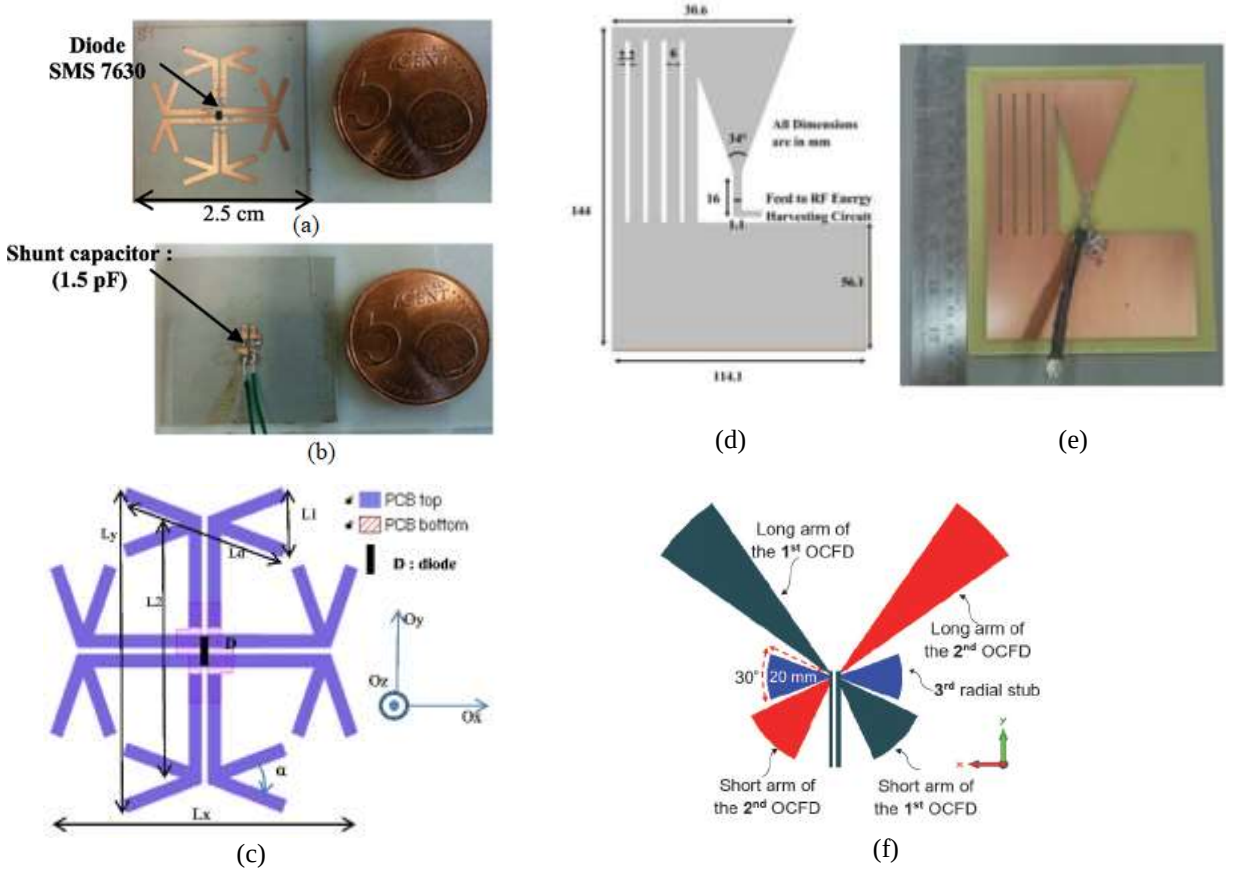

Fig. 9. Photos of the (a) top, and (b) bottom sides of the fabricated 4CDAA rectenna [60], (c) top view layout of the 4CDAA rectenna [60], (d) 5 element triangular folded monopole antenna [61] and (e) fabricated antenna [61], (f) the crossed off-center-fed bowtie dipole antenna [62].

It is stated that since the input power is high in other research, the matching circuit loss is low and its elimination is not considered necessary.

In the -20 to 0 dBm input power range, 900 MHz frequency has maximum average PCE but highest matching circuit loss. Conversely, in the 5.8 GHz frequency band matching circuit is almost lossless but PCE is not acceptable. So, for compromising between PCE and matching circuit loss, the frequency of 2.4 GHz is selected as the best choice.

In the overall conclusion, it is stated that since the matching circuit loss is dominant in low input power conditions, it should be eliminated.

In the absence of a matching circuit, for the design of a conjugate matched antenna, it is shown that the antenna should have a high inductive impedance. Widely used patch antennas have poor radiation efficiency in these conditions, so an inductively coupled feeding structure consisting of a meandered dipole and a rectangular loop is proposed and implemented (Figs. 10a, 10b and 10c). A rectangular loop is designed to match the imaginary part while the meandered dipole is designed to match the real part of the input impedance of the half-wave rectifier. This rectenna is compared to other with-matching circuit rectennas in the literature and it is shown that the proposed rectenna has the highest PCE in the low input power range which is the range of interest in energy harvesting applications. The measured PCE with the proposed rectenna in 2.45 GHz frequency is 61.4%, 50.7% and 31.8% with -5, -10 and -15 dBm input power, respectively.

In another article by the same authors, [63], the input impedance of the rectifier and insertion loss of the matching circuit are more studied and it is concluded that for designing low-power RF energy harvesters in 900 MHz and 1.8 GHz, the matching circuit should be removed. But in 2.4 GHz, the transmission line-based impedance matching circuit on low-loss Duroid-5880 substrate is allowed.

In [64], it is stated that since the low efficiency of rectenna in low input power levels (-20 to 0 dBm) is its main limitation, the following techniques are used to improve its efficiency:

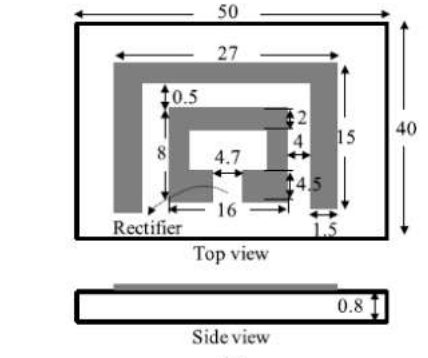

(a)

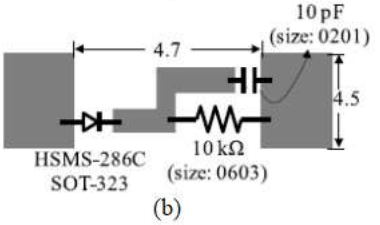

(b)

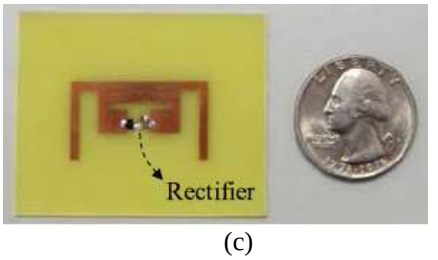

(c)

(d)

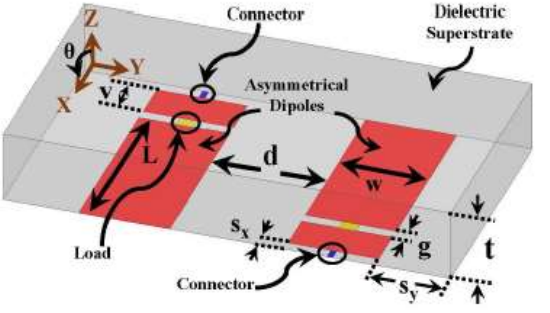

(e)

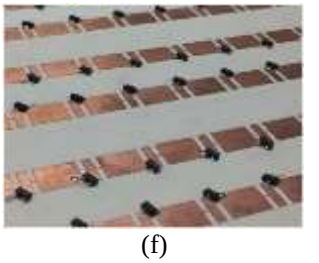

(f)

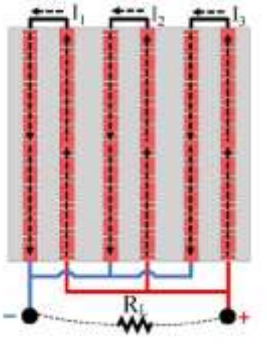

(g)

Fig. 10. (a) Layout of the optimized rectenna structure consisting of an inductively coupled feeding structure including a meandered dipole and a rectangular loop in [29], (b) layout of the rectifier, directly placed on the inductively coupled-feed loop [29], (c) prototype of the optimized rectenna structure [29], (d) slotted antipodal Bow-tie antenna, with and without slot [64], (e) unit cell of the off-center fed printed dipole energy harvesting surface with dc channeling connectors [65], (f) bottom view prototype of the planar dipole harvester surface [65], (g) dc channeling structure for the harvesting surface [65].

1) Using low loss substrate as AD600,
2) Using Greinacher topology and HSMS-2852 zero bias Schottky diode in rectifier,
3) Optimizing the impedances of the antenna and the rectifier for perfect matching at desired frequencies (0.915, 1.8 and 2.45 GHz) to avoid matching the network and its losses, by utilizing the source pull technique,
4) Increasing the amount of collected electromagnetic energy by using an omnidirectional antenna (Slotted

antipodal bow-tie antenna) (Fig. 10d). The main goal of this article is to perform source pull optimization in triple bands.

An off-center fed printed dipole as a unit cell (Fig. 10e) is designed in [65], so that its input impedance is directly matched to the rectifier (a single Schottky diode with a specific load) at a specific frequency and input power level. It is stated that since the size of the unit cell is not electrically small (as in metasurfaces), the amount of power absorbed by each unit cell is large, so the turn-on time of the diode and consequently the conversion efficiency is high. DC combining is accomplished by introducing small DC connections between 9×3 unit cells (Fig. 10f), so the DC power is channeled to the load (Fig. 10g).

In [66], a half wave rectifier in a specific operating point (load, frequency and input power) is equipped with a single open-ended stub, as a single matching element (Fig. 11a), to have a near 50 ohms input impedance. Then the standard 50 Ω rectangular patch antenna is modified and optimized (Figs. 11b and 11c) to be conjugately matched to the near 50 Ω rectifier. It is stated that the previous works (including [53] and [62]) that eliminate the matching network completely, have antennas with impedances that are far from 50 Ω, which are not so effective. Although the -20dBm input power is used as an operating condition in the optimization process and simulations in this article, experimental conditions are not clarified to be equal to this condition and should be verified. It is stated that a 56% RF-to-DC conversion efficiency is obtained when the rectenna is placed at a 10 cm distance from the 1W transmitter.

In [67], it is stated that since the ambient RF power densities in the environment are normally very low, designing a rectifier that is highly efficient over a wide range at these power levels is impossible. One way to overcome this limitation is to utilize larger electromagnetic (EM) collectors such as frequency Selective Surface (FSS) structure per rectifier (Fig. 11d). So, even at low power densities, the collected energy is large enough to drive the rectifier to its peak conversion efficiency region.

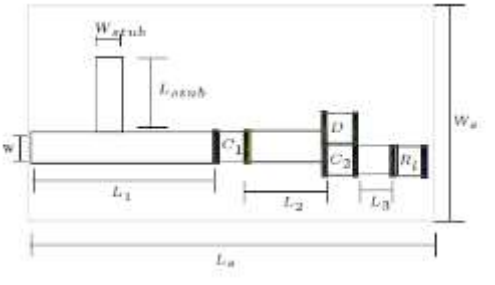

(a)

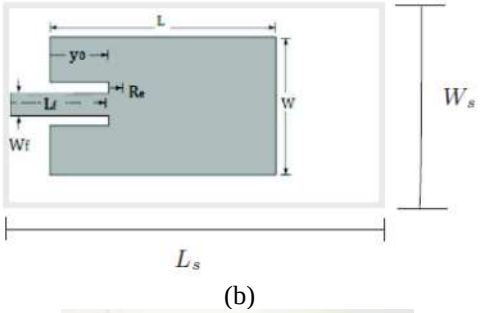

(b)

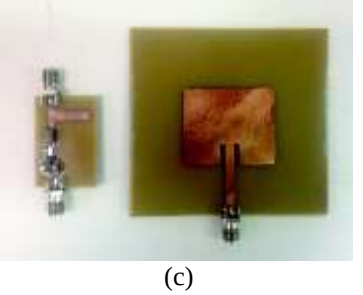

(c)

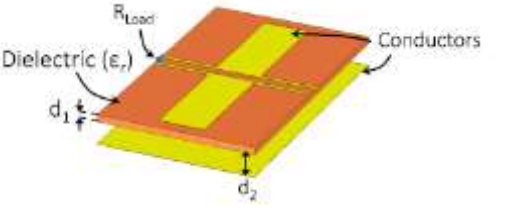

(d)

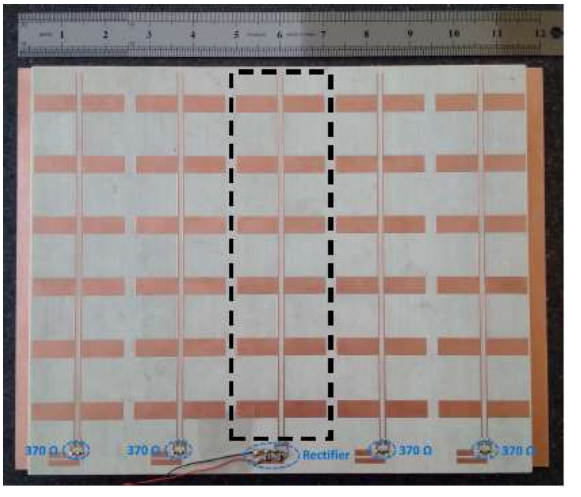

(e)

Fig. 11. (a) Matching element and rectifier circuit topology used in [66], (b) geometry of the patch antenna in [66], (c) prototype rectenna built in [66], (d) unit cell of the FSS absorber in [67], (e) rectenna consisting FSS absorber and full-wave rectifier in [67].

The FSS structure has an input impedance of 377 ohms and channels the energy to the rectifier. Integrated with the FSS structure, there is a full-wave bridge rectifier that is matched to the FSS structure using a simplified matching network (Fig. 11e). For achieving high efficiency, the full-wave bridge rectifier requires more input power than the half-wave rectifier. This higher input power level is achieved using channeling properties of the FSS structure. A different number of unit cells in the FSS structure is examined and it is concluded that although the absorption efficiency is decreased with an increasing number of unit cells, as the physical area becomes larger, the collected power at the load increases considerably, even with lower efficiencies.

In [68], a microstrip patch antenna is modified and used for direct conjugate matching to the rectifier.

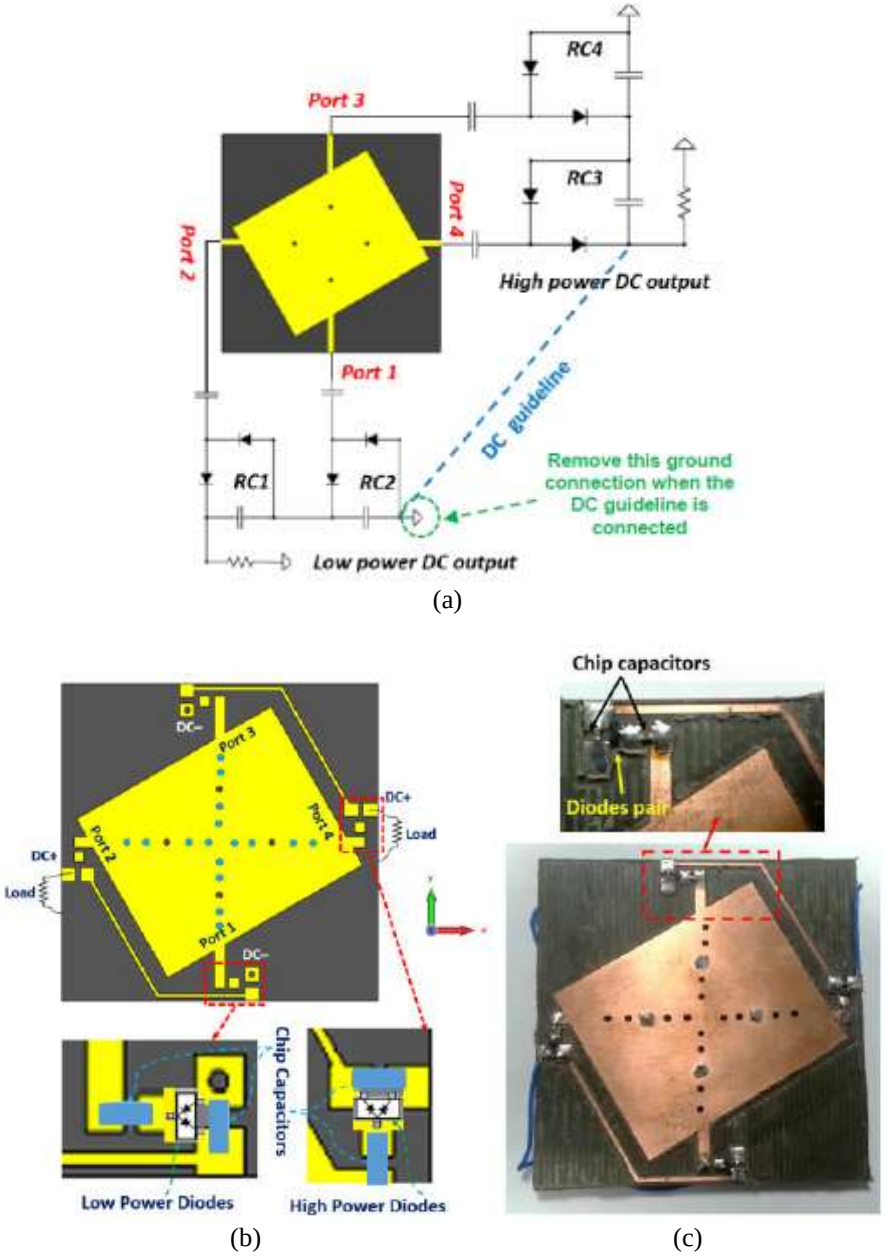

Fig. 12. (a) The rectenna design (including off-center-fed patch with two pairs of shorting pins) [68], (b) the layout of the proposed frequency-selectable rectenna (including off-center-fed patch with different shorting pins) [68], (c) the fabricated rectenna example [68].

Since the complex input impedance of the rectifier is of high values at the desired frequencies, and the high impedance of anti-resonances of the patch antenna can be used for direct matching. But the frequency bandwidth of the center-fed patch (CFP) is narrow. So, to create a multiband antenna, an off-center-fed patch (OCFP) is built by rotating the CFP around its center. This causes the current distribution on the edges of the patch to be unbalanced, which creates several resonant/anti-resonant frequencies between the CFP antenna's first and second resonant frequencies. This adds more frequencies for matching the high impedance of the rectifier. Another way to modify the current distribution on OCFP and have one more anti-resonant frequency in the desired band is by adding two symmetrical pairs of identical shorting pins on the OCFP (Fig. 12a). In this way, a total number of 4 anti-resonant high impedance frequencies in the desired band are created, which are suitable for direct matching. Also, by shifting the positions of the mentioned pins manually, these 4 frequencies can be changed, so we will have an adjustable multiband antenna suitable for direct matching to the rectifier in different frequencies (Fig. 12b).

An important point in this design is that since the matching impedances of both antenna and rectifier are of high values larger than 50 Ω, the effect of reflection coefficient variation due to impedance variation of the nonlinear rectifier is not so big compared to the standard 50 Ω system. So, this configuration is more resistant to the variation of operating conditions, and a wide range of input powers and load impedances can be used.

Another mechanism that is used for accepting multiple input polarization waves with a wide power range in this research, is to introduce three ports on other edges of the OCFP antenna, so that ports 1 and 3 are orthogonal to ports 2 and 4, respectively. Rectifiers RC1 to RC4 are connected to ports 1 to 4. If the output DC power of RC1 is combined with RC2 (and also RC3 with RC4), the rectenna can receive and rectify orthogonal polarization waves. RC1 and RC2 are tuned for low input power, while RC3 and RC4 are for higher input powers. So, a wide input power range with multiple polarizations is achieved (See Fig. 12a).

The other feature of the proposed rectenna is the insensitivity of the system to chang the types of diodes in the rectifier. This is mainly because of the high value of matching impedance as discussed above.

So, a multiband rectenna with a simple structure, that has a double polarization antenna, wide input power and load impedance range, and is relatively insensitive to the types of diodes in the rectifier is proposed in this article (Fig. 12c).

It should be mentioned that the proper impedance matching in this article is justified with relatively high rf-to-dc efficiencies obtained in a relatively high (0 to 15 dBm) input power range.

The concept of Tightly Coupled Antennas (TCA) is used in [69] with unit cells of half wavelength size. An array of unit cells, which are Vivaldi antennas (Fig. 13a), is designed such that its surface is matched to the free space wave impedance for maximizing the received AC power before channeling it to the rectifying diode. The impedance of each unit cell is adjusted to conjugately match the rectifying diode for eliminating the matching network. A simplified DC combining network is designed that uses an inductor between adjacent cells (Fig. 13b). These simplifications lead to a reduction in the total size, cost and loss of the system, in comparison with other solutions such as metamaterial arrays.

For a comparison of TCA and metasurface arrays, it is mentioned that metasurface arrays are reported to have high radiation-to-ac efficiency because of the smaller electrical size of their unit cell compared to the TCA. But the number of cells in the same area is much higher in the metasurface array than in TCA and the resonators are very close to each other. So, designing a DC combining network in metasurface arrays is a challenging task and adds extra costs and complexity to the system.

Having stated the above advantages of TCA, it is also mentioned that the metamaterial cells are better choices than TCA in applications where the footprint area of the array is constrained (such as implantable devices or remote sensing). Also, since the proposed rectenna application is limited to situations where a single normal incident wave is present, it is more appropriate for Wireless Power Transfer (WPT) than for Energy Harvesting (EH) applications, where the incoming wave direction is not known.

In [70], the hands of a clock are equipped with semi-loop and annular loop structures on a PCB to be considered as an antenna (Fig. 13c). The input impedance of a voltage doubler rectifier (Fig. 13d) and that of the mentioned antenna are simulated and matched in specific operating conditions without using any matching network. The effects of clock hands positions and annular loop radius on the antenna input impedance and radiation pattern are studied. It is concluded that proper impedance matching for specific operating conditions (frequency bands, input power level and load impedance) and conversion efficiencies over 50% can be obtained.

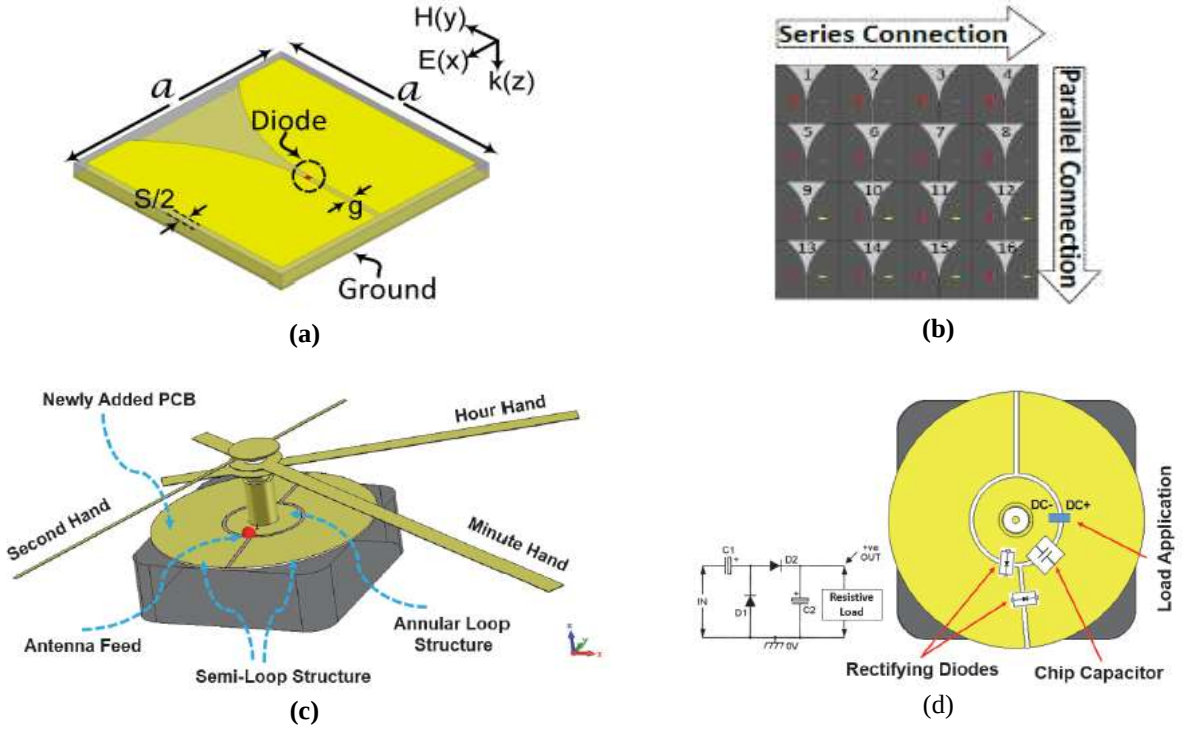

Fig. 13. (a) Unit cell of a TCA Harvester including a Vivaldi antenna [69], (b) the 4 × 4 TCA array [69], (c) a view of the clock as an antenna equipped with semi-loop and annular loop structures [70], (d) rectifier layout and its equivalent circuit [70].

2.3. Recent Works (2019-2021)

In [71], an energy harvesting surface (EHS) is designed using electrically large unit cells (compared to metasurfaces that use electrically small unit cells) and is used to increase the amount of received power per unit cell and consequently increase the turn-on time of the rectifying diode in each unit cell. Each unit cell is designed to have input impedance matched to the diode in specific operating conditions. Also, the unit cell that consists of a cross dipole antenna with a rectifying diode in each arm (Figs. 14a and 14b), is capable of harvesting energy from multiple linear polarizations (Figs. 14d and 14e). Another advantage of this work is that the DC channeling network is in the same layer of the antenna and rectifier, so there is no need for vias or an extra layer for the DC channeling network. This is done by using connecting inductors between unit cells that act as ac filters also (Fig. 14c).

Circularly polarized (CP) antennas are more likely to receive energy than linear polarized ones. So, in [72], a 2-layer CP antenna consisting of two Archimedean Spiral arms (Fig. 15a) with an Artificial Magnetic Conductor (AMC) reflector (Fig. 15b), with an air layer in between (see Fig. 15c), is designed. The antenna is conjugately matched to the rectifier for achieving more efficiency. The two spiral arms have stepped width and distance, to tune the impedance of the antenna to the rectifier at 3 different frequencies in a 400 MHz band. The AMC reflector has 3 effects: it results in a unidirectional hemispherical beamwidth, it has more bandwidth than metal reflectors, and since it is formed by four-unit cells, it acts as an FSS that has a harmonic filtering effect.

In [73], a high-power rectenna without a matching network is proposed, using an inductive folded dipole antenna (FDA) and a bridge rectifier (Fig. 15d). The complex impedance of the antenna is tuned by varying the short point place between the antenna elements (see Fig. 15e).

In [74], a Double Negative (DNG) substrate is formed by embedding high dielectric constant particles in a low dielectric constant host. Then conformed planar dipoles with a special layout are printed on the DNG substrate to make an antenna (Figs. 16a and 16b), that has good performance in gain and efficiency and also can be conjugately matched to the full wave rectifier. So, the rectenna with good performance without a matching circuit is formed. The effect of the DNG substrate is to improve the gain and efficiency of the antenna with respect to the simple substrate, and to change the antenna's input impedance, enabling it to be matched to the rectifier directly.

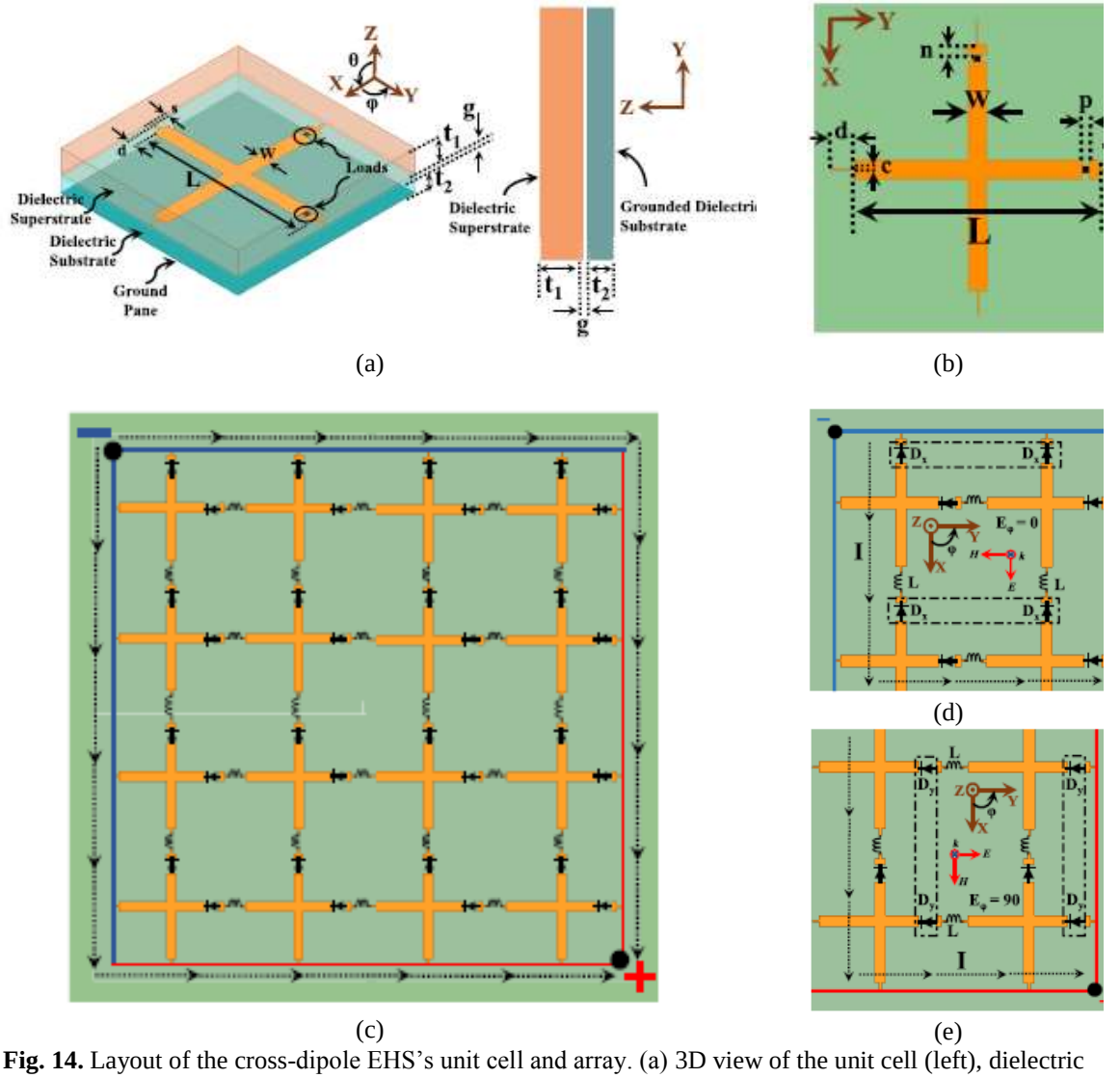

(a) (b)

(c) (d)

(e)

Fig. 14. Layout of the cross-dipole EHS's unit cell and array. (a) 3D view of the unit cell (left), dielectric layers on side view (right) (b) top view of the unit cell, (c) bottom view of 4×4 cross dipole EHS array with dc channeling structure and dc current flow, (d) D_x diodes are ON when E-field is in the X direction, (e) D_y diodes are ON when E-field is in Y direction [71].

An electrically small Huygens Circularly Polarized (HCP) antenna, which uses the concept of Near-Field Resonant Parasitic (NFRP), is designed in [75]. The antenna consists of a driven loop element and a crossed pair of balanced electric and magnetic NFRP dipole elements (see Figs. 17a to 17d).

The properties of the antenna are: circularly Polarized (CP), so there is no polarization mismatch; electrically small size, so it is compact and can be fitted into many wireless power transfer applications with Limited space; HCP antenna with a driven loop element has inductive input impedance, so it can be directly matched to a full wave rectifier which has a capacitive input impedance without using a matching network; thanks to the matching network elimination, AC to DC conversion efficiency using full wave rectifier with Schottky diodes is high (~ 90%); and the antenna has a half-power beamwidth of around 130o and gain greater than 3 dBi.

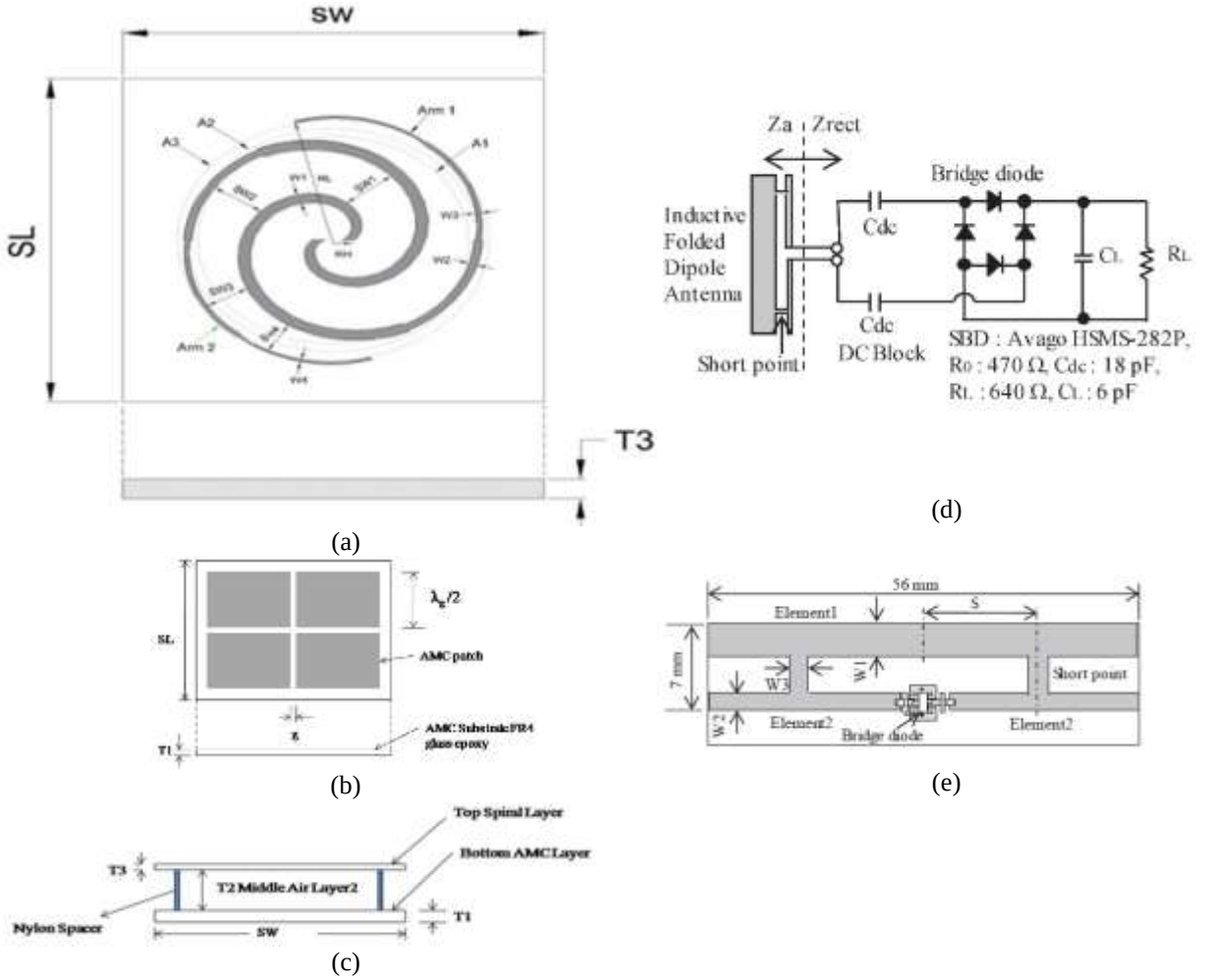

Fig. 15. (a) Top layer spiral antenna and its side view from [72], (b) bottom layer AMC and its side view [72], and (c) complete antenna side view [72], (d) circuit schematics and (e) layout of the configuration of the 2.4 GHz band rectenna consisting of inductive FDA in [73].

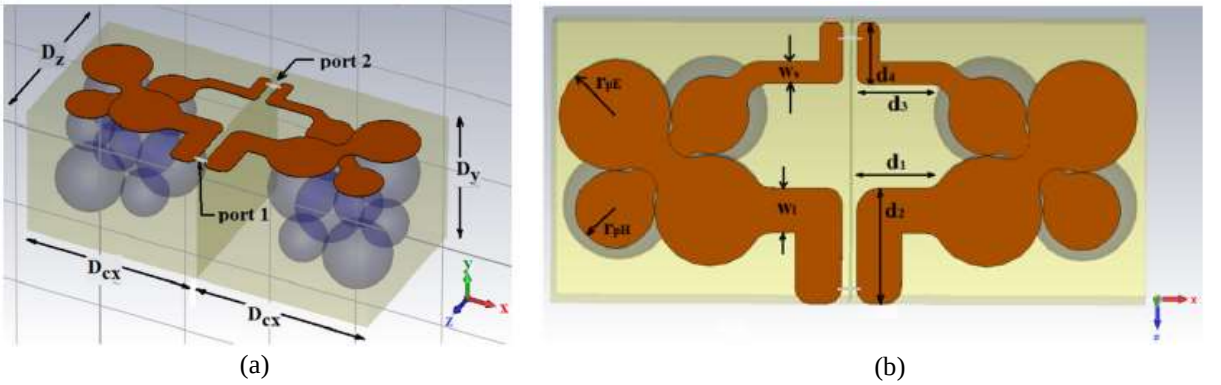

Fig. 16. (a) 3D view and (b) top view of the special planar dipole antenna printed on the DNG substrate [74].

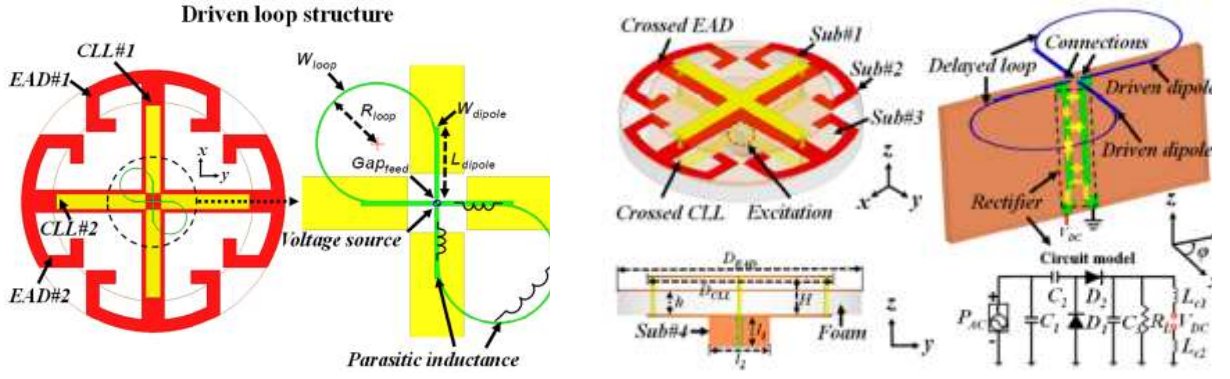

(a) (b) (c) (d)

Fig. 17. (a) Bottom view of the HCP antenna, (b) enlarged view of the driven loop element, (c) perspective view (top) and side view (bottom) of the entire HCP rectenna system, (d) layout of the vertical substrate#4 and the integrated rectifier (top), rectifier circuit model (bottom) [75].

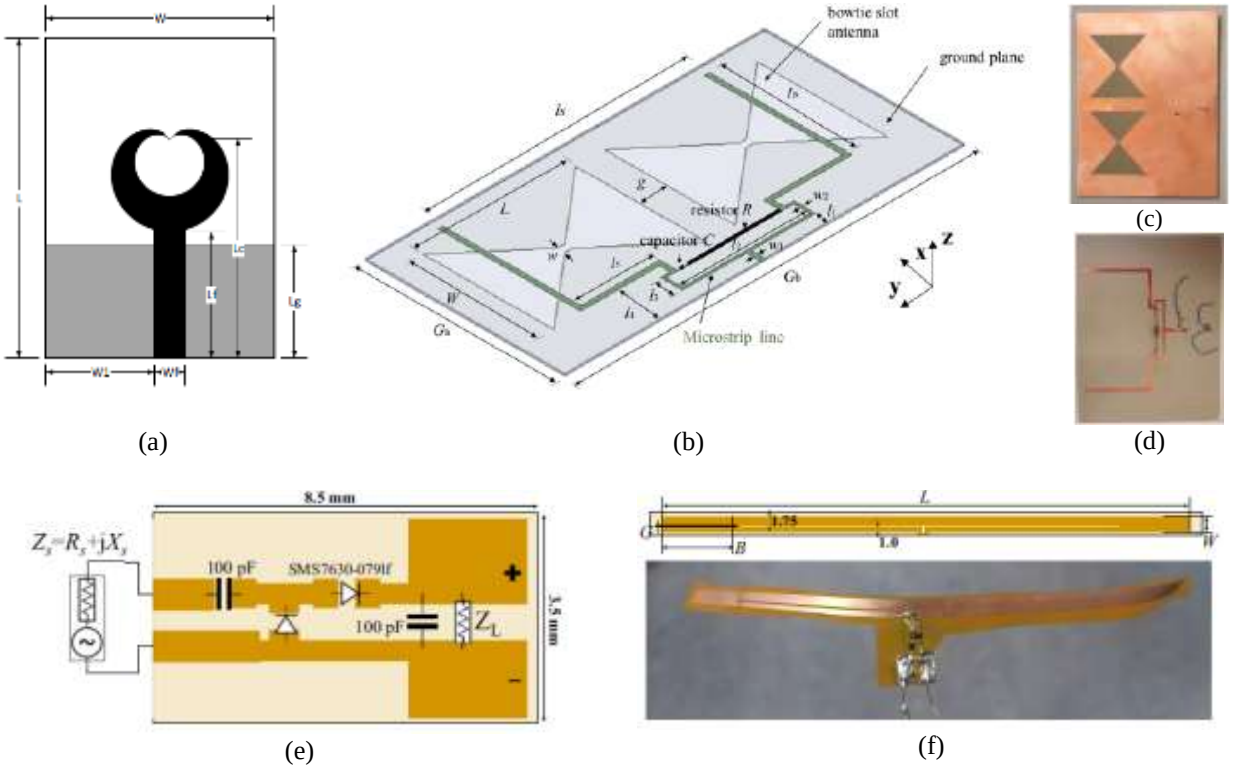

(a) (b) (c) (d) (e) (f)

Fig. 18. (a) The geometry of the fractal-based antenna in [76], (b) layout of the bowtie slot antenna in [77], (c) bottom layer of the prototype of the bowtie slot rectenna with bowtie slots etched on the ground plane [77], (d) top layer of the bowtie slot rectenna including antenna's feeding network and connected harvester [77], (e) differential voltage doubler rectifier layout from [78], (f) high-impedance FDA in [78], layout (top) and photograph (bottom).

In [76], an ultra-wideband fractal based cardioid shaped antenna on a reduced ground plane is designed (Fig. 18a). It is shown that the input impedance of this antenna is inductive over a broad range of frequencies

and so, it is roughly suitable for being directly matched to a Schottky diode with capacitive input impedance.

In [77], a mixed thermal and RF power harvester is designed. The thermal harvester dc output voltage is used to bias the Schottky diode so that its operating point shifts to the higher power conversion efficiency region. An array of two Bowtie Slot antennas that is said to be directly matched to the diode (based on the [62]) is designed and used (Figs. 18b to 18d). It is shown that the system without the matching circuit has higher efficiency than with the matching circuit.

In [78], an electrically small flexible rectenna in the sub-1 GHz band is co-designed using a voltage doubler rectifier (Fig. 18e) and a high impedance planar folded dipole antenna (FDA) (Fig. 18f). First, the rectifier source and load impedances are optimized using an iterative method to reach the maximum power conversion efficiency (PCE), then the parametric study of the antenna is performed to directly match its input impedance to the rectifier.

While in [78], the antenna's conductor was solid type and fabricated using standard photolithography on a polyimide copper-laminate, in [79] the antenna is meshed type Folded Dipole Antenna (FDA) suitable for additive manufacturing such as direct-write or screen printing, which has lower printing cost and time. Meshed-type antennas can be optically transparent and suitable for some applications such as solar cell antennas and smart displays. So, a low-resolution meshed type antenna with features larger than 1 mm is designed with high input impedance, to be directly matched with a capacitive rectifier or RFID IC (see Fig. 19a).

In [80], a technique rather than conjugate matching is used for building a small-size rectenna. An antenna consisting of two layers, each layer having a 2 by 2 array of octagonal elements, and a ground plane as a reflector are designed (Figs. 19b to 19e). It is shown that this antenna has a wide load impedance response so the efficiency of the antenna is high for a range of load impedances. In this way, it is stated that different types of diodes can be used as the rectifier without analyzing their input impedances and without using any matching circuits since the antenna load impedance response is wide. So, the rectenna is built without a matching circuit and the requirement of conjugate matching between the antenna and rectifier. Also, it is stated that by series or parallel connection of two layers, different output currents and voltage can be configured, which can be used according to the rectenna load requirements.

In [81], an asymmetrical fractal bow tie slot antenna is designed and proposed for RF energy harvesting (Fig. 20a). It is stated that an asymmetrical bow tie slot antenna, as compared to a symmetrical type, has a resonant frequency in the interested frequency band and also has an inductive input impedance, that is suitable for direct conjugate matching to the rectifier (with capacitive input impedance) in energy harvesting applications. Then, for gaining more bandwidth, while maintaining the impedance and radiation characteristics, the use of the Sierpinski fractal antenna concept is proposed. It is expressed that with this antenna design, direct matching with the rectifier is more possible, although the complete rectenna (including the rectifier circuit) is not analyzed in this article.

Antenna optimization is used in [82] to design a meander line antenna combined with spiral and folded-shaped structures (Fig. 20b), to form a small size antenna that is directly matched to the rectifier in RF energy harvesting applications. This antenna geometry is considered for both Patch Antenna (PA) and Slot Antenna (SA) (SA is the complementary structure of PA).

At the first step of the design, the geometrical parameters of the proposed antenna are swept in the allowed range by trial and error, to find the geometry for the acceptable conjugate match to a specific rectifier. This procedure is done in the CST simulator.

In the next step, the resulting geometry of the first step is used as an initial PA (IPA) to a Particle Swarm Optimization (PSO) algorithm in MATLAB together with the CST simulator, to find the Optimum PA (OPA) geometry. A fitness function is proposed to consider the reflection coefficient at the desired resonant frequency and also the lower and higher limits of the frequency band.

The resulting OPA has good performance in reflection coefficient in the resonant frequency and -3 dB impedance bandwidth, but has not good efficiency and gain performance in the desired frequencies. The complete rectenna (including the rectifier) is not analyzed in this article.

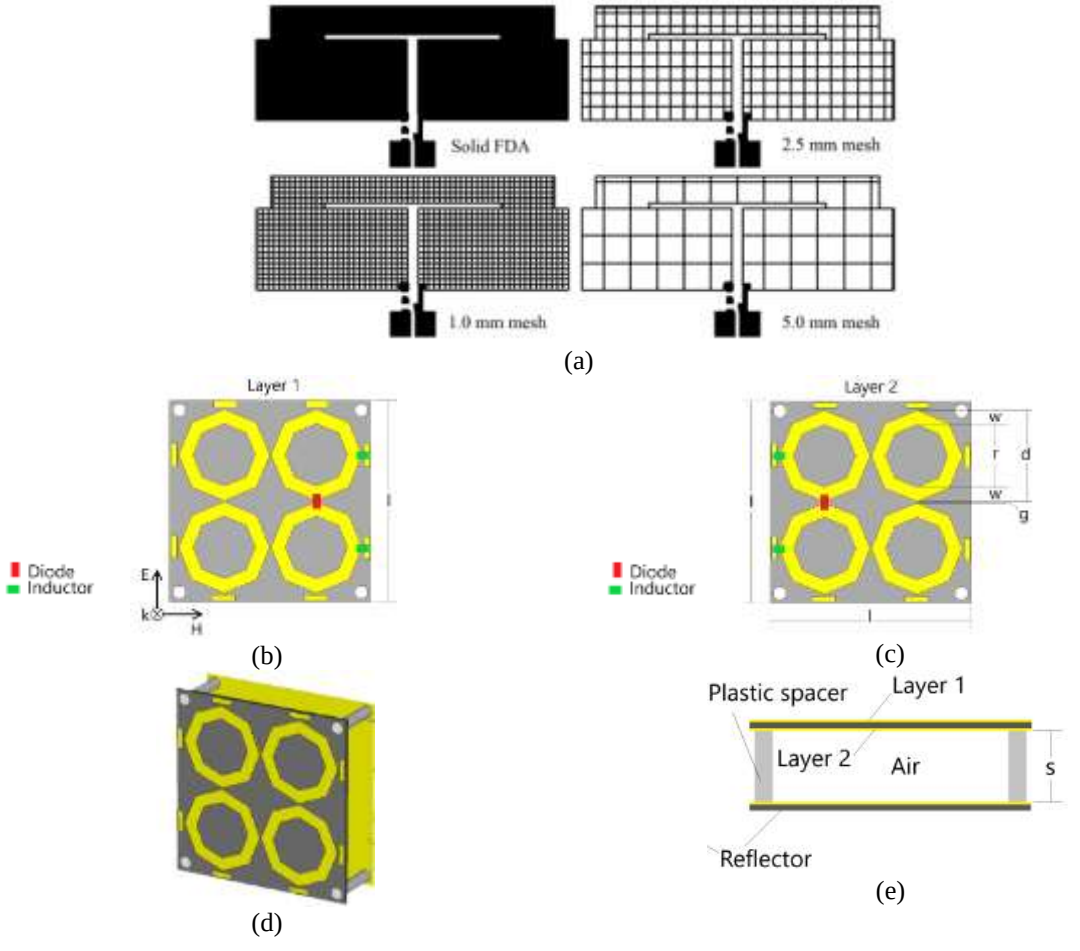

Fig. 19. (a) Layout of the meshed type FDA with different mesh spacings in [79], the array of octagonal elements in rectenna of [80], showing top views of (b) layer 1, (c) layer 2, (d) perspective view, (e) side view.

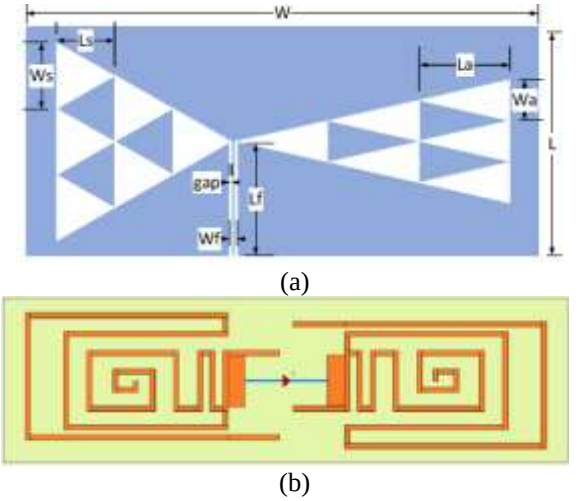

Fig. 20. (a) The geometry of Sierpinski fractal asymmetrical bow tie slot antenna [81], (b) the OPA consisting of meander line antenna combined with spiral and folded shaped structures [82].

3. COMPARISON OF SOLUTIONS

In Table 1, the key features of the above studies are mentioned as a reference to compare the research. These key features include frequency of operation, input power level, efficiency, antenna type, rectifier topology, etc.

Table 1. Key features of the reviewed articles.

Ref	Operating frequency	polarization	Matching network	Input power (density)	Efficiency (RF to DC PCE)	Output (DC power or voltage)	Antenna type	Antenna gain	Substrate	Rectifier topology	Rectenna configuration	Rectifier element (diode)	Band (single, multi, ...)	size	application	remarks
[43]	4.5 to 8 GHz 8.5 to 15 GHz	two orthogonal LP RHCP and LHCP			35% at 5.7 GHz, 7.78mW/cm² input 45% at 18.7 GHz, 1.5mW/cm² input	Max open ckt voltage 3.5 V Max open ckt voltage 4 V -12.1dBm Hor. Pol -8.32dBm Vert. Pol 1.6dBm Dual Pol	dense grid array self-similar spiral array		Duroid εr = 2.2	Diode mesh	DC combining	MA4E2054A	Wideband	9.5λ² 5λ²		160 diodes per λ² 3 diodes per λ²
[44]	2 to 18 GHz	Dual CP		10^{-5} to 10^{-1} mW/cm2	0.1% at 5*10⁻⁵ mW/cm2 20% at 0.07 mW/cm2	-44 dBm at 5*10⁻⁵ mW/cm2 to 10 dBm at 10⁻¹ mW/cm2	64 element Spiral array			Diode mesh	DC combining	Alpha SMS7630-079	broadband	18.5 cm × 18.5 cm	powering of low-power indoor sensor networks and RF Energy Recycling	Using source-pull
[45]	915 MHz 865-868 MHz		reactive shorting stub and double inductive arch				S-Shaped Folded dipole and Inductively coupled feed antenna	2.13 dBi 1.99 dBi	flexible 4-mil Liquid Crystal Polymer (LCP)					2nd antenna: 1.7in × 1.4in	RFID	
[46]	910 MHz						meandered slot dipole antenna	2.17 dBi						90-34 mm²	RFID	
[47]	2.45 GHz		Input and output radial stubs	0 dBm	40 %	0.75 V	Microstrip probe-feed patch antenna		FR4			HSMS-2852				$R_{DC Load}$=470 Ω
[48]	2.45 GHz			0 dBm	52 %	0.510 µW	Microstrip edge feed patch antenna		FR4	Voltage doubler		HSMS-2852			Electric wall clock	$R_{DC Load}$=900 Ω
[49]	2.45 GHz			0 dBm			Wire folded dipole array antenna					HSMS-2850				Z_{load} = 70.7 − j84.5 Ω
[50]	2.45 GHz						Meandered slot antenna	2.25 dB	Rogers RT/Duroid 5880 PCB				single	24 mm x 24 mm x 0.8 mm	RFID	Z_{ANT} = 15 − j250 Ω
[51]	1.5754 GHz			0-3 dBm	71 % at -4 dBm 84.7 % at 3 dBm		MTM inspired NFRP combined with 2-case monopole	1.863 dB	Duroid 5880	Single diode		SMS7630	Single (GPS L1)	Ka=0.611	GPS	Antenna impedance 29.5 + j 171.55 Ω
[52]	1.96 GHz	Single and dual LP		25-200W/cm² 0-15 dBm	43-54 %	-1.64 dBm at 0 dBm input 8.1 dBm at 15 dBm input	patch antenna		Rogers 4350 B	Single diode		SMS7630-79	Single (narrowband)		RFID	optimal impedance 337-1149 Ω
[53]	2.45 GHz		Stub	-30 to 15 dBm	80.3 % at 1.95 µW/cm² input 58 % at 8.22 µW/cm² (-17.2 dBm) input (with 1400 Ω resistor)	1 V for input power of -3.2 dBm	X-shape antenna with tuning stub	8.4 dBi	RT/Duroid 6002	Single diode		HSMS-2852	Single			Optimal capacitor and resistor 3.3 pF and 2800 Ω
[54]	2.5 GHz				Max 52 % at 10 dBm input and 300 Ω load	3.5 V at 10 dBm input and 820 Ω load	circular sector antenna		RT/Duroid 5880	Double diode		HSMS-2850	Single	19.8 x 19.8 x 1.6 mm³	WSN, micro robot	
[55]	868 MHz	horizontally polarized	Capacitor Bank	-37~-12 dBm	40 % at -17 dBm	1 V at -27 dBm input	square loop antenna with additional short-circuited arms	0.659 dBi	GML 1000	Multistage CMOS		standard TSMC 90 nm CMOS	Single	51 mm x 41 mm x 0.5 mm	WSN networks	
[9]	915 MHz, 2.45 GHz	Linear Vertical Pol	CPS stubs and a capacitor in 915 MHz	1 µW/cm² -13.5dBm@915 -11dBm@2.45	40.7 % @ 915 MHz 36.2 % @ 2.45 GHZ	11.6 µW (-19.4dBm) @ 915 MHz 65.6 µW (-11.8dBm) @ 2.45 GHz Both @ 2.2 KΩ load	three-element Yagi-Uda antenna with inductive feed	-3 dBi @ 915 8 dBi @ 2.45	flexible Rogers Ultralam 3850	Single diode		SMS7630-079			IoT	2.2 KΩ load
[56]	900 MHz			8 µW/cm²	40.6%	0 dBm	Coplanar dipole antenna with compact meandered feed line	2.2 dBi	Flexible polyethylene terephthalate (PET)			Skyworks Schottky Diode		155 × 46 × 0.13 mm³	RFID	1 KΩ DC load
[57]	868 MHz			-20 ~ 0 dBm	55% @ -10 dBm 34% @ -20 dBm		printed loop-like antenna with additional arms		1.6 mm thick FR4 substrate	Voltage doubler		HSMS2852	single			10 KΩ load
[8]	2.45 GHz		Inductive feed	1 µW/cm²	Minimum of 39% at 1 µW/cm²	15.05 µW for VDI ZBD 10.05 µW for 7630	a folded dipole with an inductive feed and a corner reflector	7.48 dBi	25-mil thick RT/Duroid 6010.2LM	Single shunt diode		VDI ZBD SMS7630-079	single		low-energy electronic applications	2.2 KΩ load
[58]	0.85 to 1.94 GHz	Horizontal and vertical		0 to 10 dBm	60 % @ 900 MHz 17 % @ 1800 MHz	2.76 V for open circuit 1.38 V across 4.7kΩ load, using the array of two rectennas when simultaneously all bands are received.	broad band bent triangular monopole antenna	Minimum of 2 dBi	FR4	Voltage doubler		Schottky diode	broadband			500 Ω load
[59]	2.60 GHz	Single linear		-8 to 10 dBm			Folded dipole array	1.73 dBi	RO4003 Rogers	single	DC combining	HSMS2860	single	138 × 220 × 300 mm³		4*4*4 antenna, 200, 500, 3900 Ω load
[60]	12, 17.6 and 20.2 GHz	Linear	Coplanar Strip Line (CPS)	30 V/m to 51 V/m electric field	12 % at 17.6 GHz 20 % at 20.2 GHz 37 % at 12 GHz and 38 V/m input Electric field Max 41 % at 12 GHz and 51 V/m input electric field	1 mW at 12 GHz and 38 V/m input electric field	four-cross-dipole antenna array	11.7 to 12.7 dBi	Rogers RT/Duroid 6002	single		SMS7630	multiband	25×25 mm² (λ² at 12 GHz)	Satellite	R_L=300 Ω
[61]	0.8 to 2.5 GHz			-12.7 to -5 dBm		0.13 V @ -12.7 dBm at 844 MHz, boosted to 3.1 V 0.47 V @ -5.7 dBm at 1.75 GHz boosted to 4.27 V	planar broadband folded dipole antenna	more than 1.5 dBi	1.6mm thick FR4	Dickson voltage doubler		Schottky Diode	broadband	~115 ×180 mm² antenna		5 KΩ load
[62]	0.9 to 1.1 GHz 1.8 to 2.5 GHz	dual		0 to 20 dBm	maximum 60% at 0 dBm, 65% at 5 dBm, 70% at 10 dBm, and 75% at 20 dBm for using the SMS7630, HSMS2850, HSMS2860, and HSMS2820 respectively		Crossed off-center-fed bowtie dipole	1.8 dBi at 0.9 GHz, 1.5 dBi at 1.8 GHz and 1.3 dBi at 2.4 GHz	Rogers RO3002	single shunt diode		SMS7630, HSMS2850, HSMS2860, and HSMS2820	broadband	120 ×120 mm²	cellular mobile, WLAN and ISM bands	200 to 2000 Ω optimal load

Table 1. (Continued) Key features of the reviewed articles

Ref	Operating frequency	polarization	Matching network	Input power (density)	Efficiency (RF to DC PCE)	Output (DC power or voltage)	Antenna type	Antenna gain	Substrate	Rectifier topology	Rectenna configuration	Rectifier element (diode)	Band (single, multi, ...)	size	application	remarks
[29]	0.9, 1.8, 2.45 and 5.8 GHz		LC network, Single-stub tuner, Double-stub tuner	-20 to 0 dBm	61.4%, 30.7%, and 11.8% at -5, -10, and -15 dBm (@ 2.45 GHz)		Inductively coupled-fed meandered dipole antenna		FR4 and Rogers Duroid 5880	Half-wave rectifier, Single-stage voltage multiplier, Greinacher charge pump, Dickson charge pump		HSMS-286C	Single band			Optimal config: FR4 substrate, freq = 2.45 GHz, half-wave rectifier with optimal load of R_L = 9 KΩ, C_j = 0pF, with no matching circuit
[44]	0.915, 1.8, 2.45 GHz			-20 to 0 dBm	7.1 (1% at -20 dBm (@ 0.915 and 1.8 GHz) Max 30.5% at 0 dBm (@ 0.915 GHz) Max 2.1% at 0 dBm (@ 1.8 GHz)		Slotted unipolar bow-tie antenna	1.92 to 2.23 dB	ADS600	Greinacher voltage doubler		HSMS-2852	Multiband	60x40x 0.8mm		30 KΩ optimal Load
[45]	3.4 GHz			3 to 120 mW	70% at 27 mW (@ 3.4 GHz)		Off-center fed dipole array		Rogers 5880 substrate Rogers TMM-10i superstrate	Single diode per unit cell	DC combining	HSMS2860	Single band	111.2 mm × 111.2 mm		array of 9×3 unit cells 2 KΩ Load
[46]	2.45 GHz		Open circuit Stub/shunt	-10 to 0 dBm (Optimization at -20 dBm)	30.4% at 10 cm distance from center with 50dBm output power	1.243 mV at -20 dBm input power	Rectangular patch antenna	3.86 dB	FR4	Half-wave rectifier		HSMS2860	Single band	80×20mm rectifier 75×75 mm antenna		1 KΩ Load
[47]	2.45 GHz	Linearly Polarized	Simple LC network	-15 to 25 dBm	67% at 15 dBm (@ 2.2 GHz)		FSS structure		Rogers RO4003C	Full-wave bridge rectifier	AC combining	HSMS2860	Single band	228 to 104.8 mm		Array of 5×6 unit cells
[48]	4 frequency band (w.1 to 2.7 GHz range	Dual orthogonal polarization		0 to 15 dBm	More than 60% Max 85% at 12 dBm (@1.85 GHz) and 2KΩ load		Tunable pin loaded off-center-fed patch antenna		Duroid 5880	voltage doubler	DC combining	HSMS2852/ HSMS2862	Multiband	90x90x 1.58 mm		800 to 4000 Ω Load
[49]	2.44 GHz	Normal incident Single polarized		0 to 350 mW	65% at 75 mW (@2.75 GHz)		TCA with 19-cell unit-cell	2.9 dB	RT5880 Rogers	Single Shunt diode	DC combining	HSMS2860	Single band	200×200 ×1.575 mm		Array of 4×4 unit cells 250 Ω Load
[50]	1.8-2.5, 3.9-2.1 and 2.4-2.9 GHz Bands			0 to 12 dBm	Max 65% at 10 dBm (@ 2.45 GHz)		Circle Shaped equipped with PCB		Duroid5880	voltage doubler		HSMS2850	Multiband			1000 Ω Load
[51]	3 GHz	Multiple Linear Polarizations		Larger than 10 dBm	Max 74% at 22.5 dBm/m²@ 3 GHz)		Cross-dipole array		Rogers TMM-10 RT/Duroid 5880	Single diode	DC combining	HSMS2860	Single band	140×140 mm	Wireless Power Transfer	Array of 7×7 unit cells 600 Ω Load
[52]	2.1, 2.5, 2.7 GHz	Circular Polarization			60% antenna efficiency		2-unit Spiral antenna with AMC reflector	4.5 to 6 dB	Taconic TLX09 FR4				Wideband	65×45 mm		270° antenna beamwidth
[53]	2.4 GHz			0 to 30 dBm	80.9% at 27 dBm (Best Efficiency@Lowest)		Inductive FDA		MAGTRON7	Bridge Rectifier		HSMS-2820	Single band	50×7 mm	Wireless Power Transfer	
[54]	1.92-2.17 GHz	Multiple Linear Polarizations		0.2 mW	Mean antenna efficiencies 49% dipole1 and 58% dipole2	50 μW for dipole 1 and 65 μW for dipole2	Spiral Layout Planar Dipole printed on (SN) Substrate		ε_r = 400 t_s = 2.00	Full-wave Rectifier		HSMS280C	Single Band	30.56× 14.70× 14.70 mm		
[55]	915 MHz	Circularly Polarized		-5.0 to 15 dBm	AC to DC conversion efficiency of 50.6% @ 10 dBm	7.5 @ 915.5 MHz and 10 dBm captured power	RCP antenna with a driven loop element	> 3 dBic	Rogers 5880	Full-wave Rectifier		HSMS2860	Single Band		Wireless Power Transfer	115° antenna beamwidth
[56]	4 to 10 GHz	Circularly Polarized			Antenna efficiency up to 80%		Fractal-based Cantor-set shaped antenna with reduced ground plane	Up to 5 dBi	FR4	Single diode		SMS7630	Ultra-wideband	18.5 × 25 × 1.6 mm		
[57]	2.4 GHz			-45 to -25 dBm	RF-to-DC efficiency 31.6% and 10.3% at -10 dBm and -40 dBm input power (both thermal and RF) respectively	0.254 μW at -20 dBm input power	Bowtie Slot Antenna	5.07 dBi	Rogers RT/Duroid 6002	Single diode		SMS7630	Single Band	35 × 110 × 0.508 mm		3.6 KΩ load, Mixed thermal and RF power harvester
[58]	0.1-900 MHz				45% at -20 dBm, 70% at -10 dBm, 85% at -5 dBm (@868 MHz)	1 V DC @ -5 dBm input, 868 MHz (across optimal load)	Planar folded dipole		Flexible Polyimide	Voltage doubler		SMS7630-079LF	Single band	(1.0.22x)		20 KΩ optimal load
[59]	915-960 MHz			-11 to 15 dBm	65% at S = 0.01 μW/cm2 (for 70% transparent antenna, i.e., 2.5 mm mesh spacing)	0.55 V,DC @ 0.01 μW/cm2 (for 70% transparent antenna, 7 KΩ load)	Meshed planar folded dipole	1.83 dBi	Kapton polyimide	Voltage doubler		SMS7630-079LF	Single band	(0.2.12) F		
[60]	2.1 GHz			20 dBm/m²	50% @ 2.1 GHz, 20 dBm/m2 and 200 Ω load	1.007 V across 950 Ω load in series connection	2-layer array of octagonal elements	7.46 dBi	RT/Duroid 5880 Rogers	Single diode		SMS7621-011LF	Single band	5mC mm²		300 to 500 Ω diode input impedance
[61]	18.2-19 GHz						Simple-slot (twist asymmetrical bow-tie slot antenna		FR4				Multiband	68.95 mm × 26.74 mm		
[62]	2.4-2.5 GHz						Meander, spiral and Double-folded patch antenna	-9 dB	FR4	Single diode		HSMS-286C	Broadband	12.8 × 9.7 × 0.8 mm²		-5 dB-F impedance Bandwidth from 2.4 to 2.49 GHz, Γ = 15 dB at 2.45 GHz

As can be seen in the table, there are considerable efforts in designing rectennas working in different frequency bands, multiple polarization of incoming waves, different input power levels, antenna and rectifier topologies, substrate material and so on. The mentioned parameters are presented in table 1 for comparison of works.

4. DISCUSSION

Although general rectenna systems have a relatively simple structure, there are some challenges in their design, which should be clearly understood to enable the designing of efficient systems. As it can be learned from literature, we may face the following issues:

- For maximum power transfer from the antenna to the rectifier, normally a matching circuit is used in between. But the matching circuit itself introduces some losses that cannot be neglected especially in low power conditions. This is the first challenge that should be addressed and one of the mentioned solutions is to remove the matching network from the circuit and use direct matching antennas.

- Rectifying diodes are nonlinear devices whose input impedance varies with input power. So, if a matching circuit is designed and used according to the predetermined rectifier input impedance, and inserted between the antenna and rectifier, the input impedance of the rectifier will be different after inserting the matching circuit, since the input power to the rectifier will be changed. So, the matching circuit should be

designed again according to the input impedance of the rectifier after inserting the matching circuit. This introduces a difficulty in matching circuit design and suggests eliminating the matching circuit from the system and designing an antenna with an impedance that is directly matched to the rectifier.

- So, removing the matching circuit helps simplify the design procedure, and reduce the size, cost and losses associated with it, but requires designing non-50 Ω antennas that their gain and efficiency are not as good as standard 50 Ω antennas. This will reduce the system's performance.

- One of the solutions to the problem of low antenna gain is to use large antennas, but this will be in contrast to the requirement of small-size rectennas. So, designing small-sized antennas with acceptable performance, such as metamaterial-inspired antennas, can be considered for new rectenna systems.

5. CONCLUSION

A review of antennas in rectennas without a matching network is done. Different antenna types and topologies for the mentioned rectennas have been the subject of research in recent years, which include standalone and array antennas with some of them inspired by metamaterials. Removing the matching circuit is a key element in these designs since it has the benefits of simplicity in the rectenna design procedure, reduction in the loss, cost, weight and size of the system and yields more efficiency especially in low power conditions.

REFERENCES

[1] William C. Brown, "**Rectenna Technology Program: Ultra-light 2.45 GHz rectenna 20 GHz rectenna**," *Report Number NAS 1.26:179558*, NASA 1987.

[2] M. Fantuzzi, "**Design and Modelling of Wireless Power Transfer and Energy Harvesting Systems**," *PhD Dissertation*, University of Bologna, Italy, 2018.

[3] S. Selvan, M. Zaman, R. Gobbi and H. Y. Wong, "**Recent advances in the design and development of radio frequency-based energy harvester for powering wireless sensors: a review**," *Journal of Electromagnetic Waves and Applications*, 32:16, pp. 2110-2134, 2018, doi: 10.1080/09205071.2018.1497548.

[4] B. Sri HarshaVardhan, R. Jagadeesh Chandra Prasad and S. Natarajamani, "**Design of Rectifier at ISM Band for RF Energy Harvesting of Low Powers**," *in 2019 International Conference on Communication and Signal Processing (ICCSP)*, 2019, pp. 0282-0285, doi: 10.1109/ICCSP.2019.8697979.

[5] [5] M. Prauzek, J. Konecny, M. Borova, K. Janosova, J. Hlavica, and P. Musilek, "**Energy Harvesting Sources, Storage Devices and System Topologies for Environmental Wireless Sensor Networks: A Review**," *Sensors*, Vol. 18, No. 8, p. 2446, Jul. 2018, doi: 10.3390/s18082446.

[6] V. Kuhn, C. Lahuec, F. Seguin and C. Person, "**A Multi-Band Stacked RF Energy Harvester With RF-to-DC Efficiency Up to 84%**," *IEEE Transactions on Microwave Theory and Techniques*, Vol. 63, No. 5, pp. 1768-1778, May 2015, doi: 10.1109/TMTT.2015.2416233.

[7] U. Muncuk, K. Alemdar, J. D. Sarode and K. R. Chowdhury, "**Multiband Ambient RF Energy Harvesting Circuit Design for Enabling Batteryless Sensors and IoT**," *IEEE Internet of Things Journal*, Vol. 5, No. 4, pp. 2700-2714, Aug. 2018, doi: 10.1109/JIOT.2018.2813162.

[8] I. Ramos and Z. Popović, "**A compact 2.45 GHz, low power wireless energy harvester with a reflector-backed folded dipole rectenna**," *in 2015 IEEE Wireless Power Transfer Conference (WPTC)*, 2015, pp. 1-3, doi: 10.1109/WPT.2015.7140159.

[9] R. Scheeler, S. Korhummel and Z. Popovic, "**A Dual-Frequency Ultralow-Power Efficient 0.5-g Rectenna**," *IEEE Microwave Magazine*, vol. 15, no. 1, pp. 109-114, Jan.-Feb. 2014, doi: 10.1109/MMM.2013.2288836.

[10] C. Song, Y. Huang, J. Zhou, J. Zhang, S. Yuan and P. Carter, "**A High-Efficiency Broadband Rectenna for Ambient Wireless Energy Harvesting**," *IEEE Transactions on Antennas and Propagation*, Vol. 63, No. 8, pp. 3486-3495, Aug. 2015, doi: 10.1109/TAP.2015.2431719.

[11] J. A. Hagerty, F. B. Helmbrecht, W. H. McCalpin, R. Zane and Z. B. Popovic, "**Recycling ambient microwave energy with broad-band rectenna arrays**," *IEEE Transactions on Microwave Theory and Techniques*, Vol. 52, No. 3, pp. 1014-1024, March 2004, doi: 10.1109/TMTT.2004.823585.

[12] C. Mikeka, and H. Arai, "**Design Issues in Radio Frequency Energy Harvesting System,**" *Sustainable Energy Harvesting Technologies - Past, Present and Future*, London, United Kingdom: IntechOpen, 2011 [Online]. Available: https://www.intechopen.com/chapters/25376 doi: 10.5772/25348.

[13] N. Shariati, "**Sensitive ambient RF Energy harvesting**," *Ph.D dissertation*, School of Engineering, RMIT University, Melbourne, Australia, 2015, Available Online: https://researchrepository.rmit.edu.au/esploro/outputs/9921864064801341.

[14] K. Niotaki, A. Georgiadis, A. Collado and J. S. Vardakas, "**Dual-Band Resistance Compression Networks for Improved Rectifier Performance**," *IEEE Transactions on Microwave Theory and Techniques*, Vol. 62, No. 12, pp. 3512-3521, Dec. 2014, doi: 10.1109/TMTT.2014.2364830.

[15] C. Felini, M. Merenda and F. G. Della Corte, "**Dynamic impedance matching network for RF energy harvesting systems**," *in 2014 IEEE RFID Technology and Applications Conference (RFID-TA)*, 2014, pp. 86-90, doi: 10.1109/RFID-TA.2014.6934206.

[16] C. Song, Y. Huang, P. Carter, J. Zhou, S. Yuan, Q. Xu and M. Kod, "**A Novel Six-Band Dual CP Rectenna Using Improved Impedance Matching Technique for Ambient RF Energy Harvesting,**" *IEEE Transactions on Antennas and Propagation*, Vol. 64,

No. 7, pp. 3160-3171, July 2016, doi: 10.1109/TAP.2016.2565697.

[17] Y. E. Sun, N. M. Mahyuddin, "**A 1.8 GHz and 2.4 GHz Multiplier Design for RF Energy Harvester in Wireless Sensor Network**," *in 9th International Conference on Robotic, Vision, Signal Processing and Power Applications, Lecture Notes in Electrical Engineering*, Vol. 398, 2017, Springer, Singapore, doi: 10.1007/978-981-10-1721-6_54.

[18] Z. Hameed, K. Moez, "**Design of impedance matching circuits for RF energy harvesting systems**," *Microelectronics Journal*, Vol. 62, pp. 49-56, 2017, doi: 10.1016/j.mejo.2017.02.004.

[19] S. Shen and R. D. Murch, "**Impedance Matching for Compact Multiple Antenna Systems in Random RF Fields**," *IEEE Transactions on Antennas and Propagation*, Vol. 64, No. 2, pp. 820-825, Feb. 2016, doi: 10.1109/TAP.2015.2510006.

[20] S. Chandravanshi, S. S. Sarma and M. J. Akhtar, "**Design of Triple Band Differential Rectenna for RF Energy Harvesting,**" *IEEE Transactions on Antennas and Propagation*, Vol. 66, No. 6, pp. 2716-2726, June 2018, doi: 10.1109/TAP.2018.2819699.

[21] J. Liu and X. Y. Zhang, "**Compact Triple-Band Rectifier for Ambient RF Energy Harvesting Application**," *IEEE Access*, Vol. 6, pp. 19018-19024, 2018, doi: 10.1109/ACCESS.2018.2820143.

[22] C. Song, Y. Huang, J. Zhou and P. Carter, "**Recent advances in broadband rectennas for wireless power transfer and ambient RF energy harvesting**," *in 2017 11th European Conference on Antennas and Propagation (EUCAP)*, 2017, pp. 341-345, doi: 10.23919/EuCAP.2017.7928536.

[23] T. Karataev, A. Bekasiewicz and S. Koziel, "**A novel dual-band rectifier circuit with enhanced bandwidth for RF energy harvesting applications,**" *in 2018 22nd International Microwave and Radar Conference (MIKON)*, 2018, pp. 161-164, doi: 10.23919/MIKON.2018.8405165.

[24] Y. Han, O. Leitermann, D. A. Jackson, J. M. Rivas and D. J. Perreault, "**Resistance Compression Networks for Radio-Frequency Power Conversion**," *IEEE Transactions on Power Electronics*, Vol. 22, No. 1, pp. 41-53, Jan. 2007, doi: 10.1109/TPEL.2006.886601.

[25] Z. -X. Du and X. Y. Zhang, "**High-Efficiency Single- and Dual-Band Rectifiers Using a Complex Impedance Compression Network for Wireless Power Transfer**," *IEEE Transactions on Industrial Electronics*, Vol. 65, No. 6, pp. 5012-5022, June 2018, doi: 10.1109/TIE.2017.2772203.

[26] C. Song, Y. Huang, J. Zhou and P. Carter, "**Improved Ultrawideband Rectennas Using Hybrid Resistance Compression Technique**," *IEEE Transactions on Antennas and Propagation*, Vol. 65, No. 4, pp. 2057-2062, April 2017, doi: 10.1109/TAP.2017.2670359.

[27] S. Agrawal, M. S. Parihar, P. N. Kondekar, "**A quad-band antenna for multi-band radio frequency energy harvesting circuit**," *AEU - International Journal of Electronics and Communications*, Vol. 85, pp. 99-107, Feb. 2018, doi: 10.1016/j.aeue.2017.12.035.

[28] H.J. Visser, R. Vullers, "**Far-field RF energy transfer and harvesting**," *Ch. 15 of the Book: Micro Energy Harvesting*, John Wiley & Sons, May 2015, pp. 321-344, ISBN (Electronic): 9783527672943.

[29] Y. S. Chen and C. W. Chiu, "**Maximum Achievable Power Conversion Efficiency Obtained Through an Optimized Rectenna Structure for RF Energy Harvesting**," *IEEE Transactions on Antennas and Propagation*, Vol. 65, No. 5, pp. 2305-2317, May 2017, doi: 10.1109/TAP.2017.2682228.

[30] J. May, "**Principles, Applications and Selection of Receiving Diodes**," *Rev. V1, AG314 Application Note*, M/A-COM Technology Solutions.

[31] A. M. H. Almohaimeed, "**Efficient Harvester with Wide Dynamic Input Power Range for 900 MHz Wireless Power Transfer Applications**," *Ph.D dissertation*, University of Ottawa, ON, Canada, 2018, Available Online: https://ruor.uottawa.ca/bitstream/10393/38070/3/Almohaimeed_Abdullah_Mohammed_H_2018_thesis.pdf

[32] Q. Zhang, J. -H. Ou, Z. Wu and H. -Z. Tan, "**Novel Microwave Rectifier Optimizing Method and Its Application in Rectenna Designs,**" *IEEE Access*, Vol. 6, pp. 53557-53565, 2018, doi: 10.1109/ACCESS.2018.2871087.

[33] S. Keyrouz, "**Practical rectennas: far-field RF power harvesting and transport**," *Ph.D dissertation*, Eindhoven University of Technology, Eindhoven, The Netherlands, 2014, doi: 10.6100/IR774472, Available Online: https://research.tue.nl/files/3922928/774472.pdf.

[34] S. Keyrouz, H. J. Visser and A. G. Tijhuis, "**Rectifier analysis for Radio Frequency energy harvesting and Power Transport,**" *in 2012 42nd European Microwave Conference*, 2012, pp. 428-431, doi: 10.23919/EuMC.2012.6459081.

[35] R. G. Harrison and X. Le Polozec, "**Nonsquarelaw behavior of diode detectors analyzed by the Ritz-Galerkin method**," *IEEE Transactions on Microwave Theory and Techniques*, Vol. 42, No. 5, pp. 840-846, May 1994, doi: 10.1109/22.293533.

[36] J. A. Hagerty, N. D. Lopez, B. Popovic and Z. Popovic, "**Broadband Rectenna Arrays for Randomly Polarized Incident Waves**," *in 2000 30th European Microwave Conference*, 2000, pp. 1-4, doi: 10.1109/EUMA.2000.338757.

[37] G. Marrocco, "**The art of UHF RFID antenna design: impedance-matching and size-reduction techniques**," *IEEE Antennas and Propagation Magazine*, Vol. 50, No. 1, pp. 66-79, Feb. 2008, doi: 10.1109/MAP.2008.4494504.

[38] N. Michishita and Y. Yamada, "**A novel impedance matching structure for a dielectric loaded 0.05 wavelength small meander line antenna**," *in 2006 IEEE Antennas and Propagation Society International Symposium*, 2006, pp. 1347-1350, doi: 10.1109/APS.2006.1710795.

[39] Wonkyu Choi, H. W. Son, Chansoo Shin, Ji-Hoon Bae and Gilyoung Choi, "**RFID tag antenna with a meandered dipole and inductively coupled feed**," *in 2006 IEEE Antennas and Propagation Society International Symposium*, 2006, pp. 619-622, doi: 10.1109/APS.2006.1710600.

[40] K. V. S. Rao, P. V. Nikitin and S. F. Lam, "**Antenna design for UHF RFID tags: a review and a practical application,**" *IEEE Transactions on Antennas and Propagation*, Vol. 53, No. 12, pp. 3870-3876, Dec. 2005, doi: 10.1109/TAP.2005.859919.

[41] A. Toccafondi and P. Braconi, "**Compact load-bars meander line antenna for UHF RFID transponder**," *in 2006 First European Conference on Antennas and Propagation*, 2006, pp. 1-4, doi: 10.1109/EUCAP.2006.4584839.

[42] Chihyun Cho, Hosung Choo and Ikmo Park, "**Design of Novel RFID Tag Antennas for Metallic Objects,**" *in 2006 IEEE Antennas and Propagation Society International Symposium*, 2006, pp. 3245-3248, doi: 10.1109/APS.2006.1711303.

[43] Yuri Tikhov, Yongjin Kim and Young-Hoon Min, "**Compact low cost antenna for passive RFID transponder**," *in 2006 IEEE Antennas and Propagation Society International Symposium*, 2006, pp. 1015-1018, doi: 10.1109/APS.2006.1710705.

[44] Byunggil Yu, Sung-Joo Kim, Byungwoon Jung, F. J. Harackiewicz, Myun-Joo Park and Byungje Lee, "**Balanced RFID Tag Antenna Mountable on Metallic Plates**," *in 2006 IEEE Antennas and Propagation Society International Symposium*, 2006, pp. 3237-3240, doi: 10.1109/APS.2006.1711301.

[45] A. H. Rida, L. Yang, S. S. Basat, A. Ferrer-Vidal, S. Nikolaou and M. M. Tentzeris, "**Design, Development and Integration of Novel Antennas for Miniaturized UHF RFID Tags**," *IEEE Transactions on Antennas and Propagation*, Vol. 57, No. 11, pp. 3450-3457, Nov. 2009, doi: 10.1109/TAP.2009.2027347.

[46] J. Kim, I. Y. Oh, J. C. Kim, D. Kim, T. W. Koo and J. G. Yook, "**Design of a meandered slot antenna for UHF RFID applications**," *in 2010 IEEE Antennas and Propagation Society International Symposium*, 2010, pp. 1-4, doi: 10.1109/APS.2010.5561182.

[47] J. A. G. Akkermans, M. C. van Beurden, G. J. N. Doodeman and H. J. Visser, "**Analytical models for low-power rectenna design**," *IEEE Antennas and Wireless Propagation Letters*, Vol. 4, pp. 187-190, 2005, doi: 10.1109/LAWP.2005.850798.

[48] H.J. Visser, "**Approximate Antenna Analysis for CAD**," *Ch. 5*, John Wiley & Sons, March 2009, ISBN (Electronic): 9780470986387, URL: https://ieeexplore.ieee.org/servlet/opac?bknumber=8039953.

[49] H. J. Visser and R. J. M. Vullers, "**Time efficient method for automated antenna design for wireless energy harvesting**," *in 2010 Loughborough Antennas & Propagation Conference*, 2010, pp. 433-436, doi: 10.1109/LAPC.2010.5666213.

[50] O. Kazanc, C. Dehollain and F. Maloberti, "**Impedance-matched sensor-tag antenna design using genetic algorithm optimization**," *in 2011 5th International Symposium on Medical Information and Communication Technology*, 2011, pp. 61-64, doi: 10.1109/ISMICT.2011.5759797.

[51] N. Zhu, R. W. Ziolkowski, and H. Xin, "**A metamaterial-inspired, electrically small rectenna for high-efficiency, low power harvesting and scavenging at the global positioning system L1 frequency**," *Applied Physics Letters*, Vol. 99, pp. 114101, 2011, doi: 10.1063/1.3637045.

[52] E. Falkenstein, M. Roberg and Z. Popovic, "**Low-Power Wireless Power Delivery**," *IEEE Transactions on Microwave Theory and Techniques*, vol. 60, no. 7, pp. 2277-2286, July 2012, doi: 10.1109/TMTT.2012.2193594.

[53] H. Sun, Y. -x. Guo, M. He and Z. Zhong, "**Design of a High-Efficiency 2.45-GHz Rectenna for Low-Input-Power Energy Harvesting**," *IEEE Antennas and Wireless Propagation Letters*, vVol. 11, pp. 929-932, 2012, doi: 10.1109/LAWP.2012.2212232.

[54] T. Choi and S.-M. Han, "**Compact Rectenna System Design Using a Direct Impedance Matching Method**," *The Journal of Korean Institute of Electromagnetic Engineering and Science*, vol. 24, no. 3. Korean Institute of Electromagnetic Engineering and Science, pp. 286–291, 31-Mar-2013, doi: 10.5515/KJKIEES.2013.24.3.286.

[55] M. Stoopman, S. Keyrouz, H. J. Visser, K. Philips and W. A. Serdijn, "**Co-Design of a CMOS Rectifier and Small Loop Antenna for Highly Sensitive RF Energy Harvesters,**" *IEEE Journal of Solid-State Circuits*, Vol. 49, No. 3, pp. 622-634, March 2014, doi: 10.1109/JSSC.2014.2302793.

[56] S. Korhummel, D. G. Kuester and Z. Popović, "**A harmonically-terminated two-gram low-power rectenna on a flexible substrate**," *in 2013 IEEE Wireless Power Transfer (WPT)*, 2013, pp. 119-122, doi: 10.1109/WPT.2013.6556897.

[57] H. J. Visser, S. Keyrouz, and A. B. Smolders, "**Optimized rectenna design**," *Wireless Power Transfer*, vVol. 2, No. 1, pp. 44–50, 2015, doi: 10.1017/wpt.2014.14.

[58] M. Arrawatia, M. S. Baghini and G. Kumar, "**Broadband Bent Triangular Omnidirectional Antenna for RF Energy Harvesting**," *IEEE Antennas and Wireless Propagation Letters*, Vol. 15, pp. 36-39, 2016, doi: 10.1109/LAWP.2015.2427232.

[59] T. S. Almoneef, H. Sun and O. M. Ramahi, "**A 3-D Folded Dipole Antenna Array for Far-Field Electromagnetic Energy Transfer,**" *IEEE Antennas and Wireless Propagation Letters*, Vol. 15, pp. 1406-1409, 2016, doi: 10.1109/LAWP.2015.2511183.

[60] A. Okba, A. Takacs, H. Aubert, S. Charlot, P. F. Calmon, "**Multiband rectenna for microwave applications,**" *Comptes Rendus Physique*, Vol. 18, No. 2, pp. 107-117, 2017, doi: 10.1016/j.crhy.2016.12.002.

[61] M. Arrawatia, M. S. Baghini and G. Kumar, "**Broadband RF energy harvesting system covering CDMA, GSM900, GSM1800, 3G bands with inherent impedance matching**," *in 2016 IEEE MTT-S International Microwave Symposium (IMS)*, 2016, pp. 1-3, doi: 10.1109/MWSYM.2016.7540144.

[62] C. Song, Y. Huang, J. Zhou, P. Carter, S. Yuan, Q. Xu, and Z. Fei, "**Matching Network Elimination in Broadband Rectennas for High-Efficiency Wireless Power Transfer and Energy Harvesting**," *IEEE Transactions on Industrial Electronics*, Vol. 64, No. 5, pp. 3950-3961, May 2017, doi: 10.1109/TIE.2016.2645505.

[63] Y. S. Chen and C. W. Chiu, "**Insertion Loss**

Characterization of Impedance Matching Networks for Low-Power Rectennas," *IEEE Transactions on Components, Packaging and Manufacturing Technology*, Vol. 8, No. 9, pp. 1632-1641, Sept. 2018, doi: 10.1109/TCPMT.2018.2864183.

[64] A. Lopez-Yela and D. Segovia-Vargas, "**A triple-band bow-tie rectenna for RF energy harvesting without matching network**," *in 2017 IEEE Wireless Power Transfer Conference (WPTC)*, 2017, pp. 1-4, doi: 10.1109/WPT.2017.7953809.

[65] A. Z. Ashoor, T. S. Almoneef and O. M. Ramahi, "**A Planar Dipole Array Surface for Electromagnetic Energy Harvesting and Wireless Power Transfer**," *IEEE Transactions on Microwave Theory and Techniques*, Vol. 66, No. 3, pp. 1553-1560, March 2018, doi: 10.1109/TMTT.2017.2750163.

[66] P. Pereira, R. C. M. Pimenta, R. Adriano, G. L. F. Brandão and Ú. C. Resende, "**Antenna impedance correction for low power energy harvesting devices**," *in 2017 SBMO/IEEE MTT-S International Microwave and Optoelectronics Conference (IMOC)*, 2017, pp. 1-5, doi: 10.1109/IMOC.2017.8121124.

[67] F. Erkmen, T. S. Almoneef and O. M. Ramahi, "**Scalable Electromagnetic Energy Harvesting Using Frequency-Selective Surfaces**," *IEEE Transactions on Microwave Theory and Techniques*, Vol. 66, No. 5, pp. 2433-2441, May 2018, doi: 10.1109/TMTT.2018.2804956.

[68] C. Song, Y. Huang, P. Carter, J. Zhou, S. D. Joseph and G. Li, "**Novel Compact and Broadband Frequency-Selectable Rectennas for a Wide Input-Power and Load Impedance Range,**" *IEEE Transactions on Antennas and Propagation*, Vol. 66, No. 7, pp. 3306-3316, July 2018, doi: 10.1109/TAP.2018.2826568.

[69] T. S. Almoneef, F. Erkmen, M. A. Alotaibi and O. M. Ramahi, "**A New Approach to Microwave *Rectennas Using Tightly Coupled Antennas*,**" *IEEE Transactions on Antennas and Propagation*, vol. 66, no. 4, pp. 1714-1724, April 2018, doi: 10.1109/TAP.2018.2806398.

[70] C. Song, A. López-Yela, Y. Huang, D. Segovia-Vargas, Y. Zhuang, Y. Wang and J. Zhou, "**A Novel Quartz Clock with Integrated Wireless Energy Harvesting and Sensing Functions,**" *IEEE Transactions on Industrial Electronics*, Vol. 66, No. 5, pp. 4042-4053, May 2019, doi: 10.1109/TIE.2018.2844848.

[71] A. Z. Ashoor and O. M. Ramahi, "**Polarization-Independent Cross-Dipole Energy Harvesting Surface**," *IEEE Transactions on Microwave Theory and Techniques*, Vol. 67, No. 3, pp. 1130-1137, March 2019, doi: 10.1109/TMTT.2018.2885754.

[72] D. Sabhan, V. J. Nesamoni, and J. Thangappan, "**A wide-beam, circularly polarized, three-staged, stepped-impedance, spiral antenna for direct matching to rectifier circuits**," *Review of Scientific Instruments*, Vol.90, No. 5, pp. 054704, May 2019, doi: 10.1063/1.5088572.

[73] A. Hirono, N. Sakai and K. Itoh, "**High efficient 2.4GHz band high power rectenna with the direct matching topology,**" *in 2019 IEEE Asia-Pacific Microwave Conference (APMC)*, 2019, pp. 1268-1270, doi: 10.1109/APMC46564.2019.9038304.

[74] A. Karampatea, K. Siakavara, "**Hybrid rectennas of printed dipole type on Double Negative Dielectric Media for powering sensors via RF ambient energy harvesting,**" *AEU - International Journal of Electronics and Communications*, Vol. 108, pp. 242-250, Aug. 2019, doi: 10.1016/j.aeue.2019.06.023.

[75] W. Lin and R. W. Ziolkowski, "**Electrically Small Huygens CP Rectenna with a Driven Loop Element Maximizes Its Wireless Power Transfer Efficiency**," *IEEE Transactions on Antennas and Propagation*, Vol. 68, No. 1, pp. 540-545, Jan. 2020, doi: 10.1109/TAP.2019.2935784.

[76] L. Lazović, B. Jokanovic, V. Rubežić and A. Jovanović, "**Printed Ultra-Wideband Cardioid Monopole Antenna for Energy Harvesting Application**," *in 2019 14th International Conference on Advanced Technologies, Systems and Services in Telecommunications (TELSIKS)*, 2019, pp. 134-137, doi: 10.1109/TELSIKS46999.2019.9002362.

[77] L. Guo, X. Gu, P. Chu, S. Hemour and K. Wu, "**Collaboratively Harvesting Ambient Radiofrequency and Thermal Energy**," *IEEE Transactions on Industrial Electronics*, Vol. 67, No. 5, pp. 3736-3746, May 2020, doi: 10.1109/TIE.2019.2914627.

[78] M. Wagih, A. S. Weddell and S. Beeby, "**High-Efficiency Sub-1 GHz Flexible Compact Rectenna based on Parametric Antenna-Rectifier Co-Design,**" *in 2020 IEEE/MTT-S International Microwave Symposium (IMS)*, 2020, pp. 1066-1069, doi: 10.1109/IMS30576.2020.9223796.

[79] M. Wagih, A. S. Weddell and S. Beeby, "**Meshed High-Impedance Matching Network-Free Rectenna Optimized for Additive Manufacturing**," *IEEE Open Journal of Antennas and Propagation*, Vol. 1, pp. 615-626, 2020, doi: 10.1109/OJAP.2020.3038001.

[80] T. S. Almoneef, "**Design of a Rectenna Array without a Matching Network,**" *IEEE Access*, Vol. 8, pp. 109071-109079, 2020, doi: 10.1109/ACCESS.2020.3001903.

[81] R. Čvorović, L. Lazović, V. Rubežić and A. Jovanović, "**Printed asymmetrical Sierpinski slot antenna for energy harvesting application**," *in 2020 24th International Conference on Information Technology (IT)*, 2020, pp. 1-4, doi: 10.1109/IT48810.2020.9070358.

[82] R. M. Yaseen, D. K. Naji, and A. M. Shakir, "**Optimization Design Methodology of Broadband or Multiband Antenna for RF Energy Harvesting Applications,**" *Progress in Electromagnetics Research B*, Vol. 93, pp. 169-194, 2021, doi:10.2528/PIERB21070104.